POLITECNICO DI TORINO
Repository ISTITUZIONALE

Enhancing operational performance of AHUs through an advanced fault detection and diagnosis process based on temporal association and decision rules

(Article begins on next page)

02 May 2024

Enhancing operational performance of AHUs through an advanced fault detection and diagnosis process based on temporal association and decision rules

Marco Savino Piscitelli[a], Daniele Mauro Mazzarelli[a], Alfonso Capozzoli[a*]

[a] *Dipartimento Energia "Galileo Ferraris", Politecnico di Torino, Corso Duca degli Abruzzi 24, 10129 Torino, Italy*

* Corresponding author: Tel: +39-011-090-4413, fax: +39-011-090-4499, e-mail: alfonso.capozzoli@polito.it

Abstract

The pervasive monitoring of HVAC systems through Building Energy Management Systems (BEMSs) is enabling the full exploitation of data-driven based methodologies for performing advanced energy management strategies. In this context, the implementation of Automated Fault Detection and Diagnosis (AFDD) based on collected operational data of Air Handling Units (AHUs) proved to be particularly effective to prevent anomalous running modes which can lead to significant energy waste over time and discomfort conditions in the built environment. The present work proposes a novel methodology for performing AFDD, based on both unsupervised and supervised data-driven methods tailored according to the operation of an AHU during transient and non-transient periods. The whole process is developed and tested on a sample of real data gathered from monitoring campaigns on two identical AHUs in the framework of the Research Project ASHRAE RP-1312. During the start-up period of operation, the methodology exploits Temporal Association Rules Mining (TARM) algorithm for an early detection of faults, while during non-transient period a number of classification models are developed for the identification of the deviation from the normal operation. The proposed methodology, conceived for real-time implementation, proved to be capable of robustly and promptly identifying the presence of typical faults in AHUs.

Highlights

28 • A fault detection and diagnosis process is applied on AHU monitoring data;

29 • A novel methodology tailored on transient and non-transient operation is proposed;

30 • Faults in the transient period are detected with multivariate association rules;

31 • Temporal associations are exploited during the start-up period of the system;

32 • Decision rules are extracted for fault diagnosis in non-transient regime of AHU;

1 Introduction

34 Recent years have seen an increasing interest of the scientific community in exploring solutions to

35 improve energy efficiency in buildings by implementing advanced data-analytics based energy

36 management strategies. The application of these strategies is supported by the increasing penetration

37 of ICT (Information and Communication Technologies) and EMSs (Energy Management System) in

38 buildings, which may enable the adoption of data analytics based procedures for the exploitation of

39 collected energy-related data and the extraction of hidden knowledge in an automatic way [1].

40 Building Energy Management System (BEMS) are mainly used for tracking and managing the

41 operation and energy performance over time of Heating Ventilation and Air Conditioning (HVAC)

42 systems. The optimal management of HVAC systems, which accounts in the developed countries for

43 10-20% of the total energy share in buildings [2], is a crucial task, considering that such systems

44 account for 50% of the energy demand in commercial buildings [3].

45 However, due to lack of proper maintenance, failure of components or incorrect installation, Air

46 Handling Units (AHUs) are often run in inappropriate operational conditions. A study conducted on

47   more than 55.000 AHUs, showed that a fraction of 90% of them runs with one or multiple faults [4],

48   where a fault is intended as an abnormal system state, an unpermitted deviation of at least one

49   characteristic property of the system from the acceptable, usual, standard conditions. The

50   identification and diagnosis of faults, in the case of HVAC systems, can lead to potential savings of

51   about 30% [5]. This process is also known as Fault Detection and Diagnosis (FDD) where *fault*

52   *detection* consists in the recognition of a fault occurrence, and *fault diagnosis* corresponds to the

53   identification of the causes and the location of the fault [6]. Advanced methods of *fault detection* are

54   based on mathematical models and on methods of system and process modelling to generate fault

55   *symptoms* (e.g. residuals). *Fault diagnosis* methods use causal fault-symptom-relationships by

56   applying techniques from statistical decision, artificial intelligence and soft computing [6].

57   Although currently underutilized, FDD is a powerful tool for ensuring high efficiency in building

58   operation and FDD products represent a very fast-growing market in the context of building analytics

59   technologies [7]. According to [8], over 30 FDD products are available in U.S. that may be delivered

60   through different implementation models [7]. The algorithms behind FDD tools may be integrated

61   into server-based software, desktop software, or software directly embedded in equipment controllers.

62   FDD algorithms are based on historical data that can be gathered from different sources such as

63   Building Automation Systems (BAS), equipment controllers, external sensors and meters, or mixed

64   sources. Despite the existing differences in the way tools are implemented and integrated with the

65   monitoring system, the main tool classification can be performed according to the approach employed

66   for conducting the FDD analysis.

67   The methods used for performing an FDD analysis can be classified in quantitative model-based,

68   qualitative model-based and data driven-based, as done in [9].

69   The quantitative model-based approach includes all the methods involving engineering models with

70   different levels of detail in the physical description of the system (e.g. white box models). The

71   qualitative model-based methods exploit the system knowledge derived from domain expertise (e.g.

72   rule-based, qualitative models). The last category includes data-driven methodologies exploiting

collected operational data of the system under investigation (e.g. Artificial Neural Networks, Association Rules Mining, grey box models). While rule-based methodologies (qualitative approach) are largely used, vendors are beginning to use data driven methodologies for addressing FDD tasks [7].

The next section provides an overview of the use of data-driven approach for FDD, with a specific focus to AHU systems.

1.1   Data-driven approach for FDD analysis in AHUs

In the last few years, the data-driven approach for the FDD analysis gained more and more interest, thanks to its applicability even in the case engineering models of the building and systems are inadequate or difficult to be developed, or the physics-based knowledge is not wide enough [9]. In this context, particularly promising appears the implementation of machine-learning techniques, which include both supervised and unsupervised algorithms. As pointed out in [10], the main advantages of the artificial intelligence-based data-driven approach, in comparison to traditional approaches, rely on the opportunity to:

- Learn automatically patterns from system operational data without the use of physical models. The data-driven approach does not require an a-priori understanding of the relationships that exist among faults and their symptoms.
- Achieve higher fault-detection and fault-diagnosis accuracy than qualitative methods (rules based on expert knowledge), also for faults of low severity levels.
- Perform FDD analysis exploiting a limited number of variables. It means that approach can enable an optimisation of sensor installation and then significantly reduce the number of required sensors.

More in detail, the supervised approach uses the domain expertise to develop useful prediction tool, since monitored data include variables for both input and output of the model (i.e. regression or

97 classification methods). On the other hand, the unsupervised methods (e.g., cluster analysis,

98 association-rule mining) are capable to extract hidden knowledge without a pre-defined target (i.e.

99 data used do not have any output values) and are particularly effective in case of poor-information

100 systems or when the objective of the analysis is not a-priori constrained [11].

101 The methods involving the construction of supervised estimation models mainly consider the

102 implementation of a residual analysis in order to perform an FDD process. The residual in that context

103 is the difference between the estimated and the measured value of a specific target variable: the

104 estimation is performed by means of a fault-free supervised model, while actual data may be related

105 to faulty conditions. Therefore, the residual analysis is used as a way for assessing the severity of the

106 deviation from the fault-free conditions during operation [12].

107 Many applications of supervised and unsupervised techniques for Automated Fault Detection and

108 Diagnosis (AFDD) are reported in literature, particularly for detecting faults during the non-transient

109 operation of AHUs [13].

110 Even though each component of an AHU can be potentially corrupted by a fault, the most common

111 faults can affect sensors (e.g. offset in the measurement), controlled devices (e.g. blockage or leakage

112 of air damper or coil valves), equipment (e.g. coil fouling or reduced capacity, duct leakage, fan

113 complete failure or deviation in the pressure drop or belt slippage) and controllers (e.g. unstable or

114 frozen control signal for dampers, coils or fan) [14]. In [15] was proposed a methodology to identify

115 faults related to the fans and the air dampers of an AHU. The methodology uses a Multi-Class Support

116 Vector Machine (MC-SVM), for the identification of both pre-labelled faults and new ones. In [16]

117 and [17], a Bayesian Network (BN) was adopted for the diagnosis of faults related to air dampers,

118 cooling coil valve stuck and return fan failure. The BN exploited in input the residuals obtained from

119 a set of limit-checking rules and statistical models, capable of estimating air temperature, water flow

120 rate, air flow rate and fan power consumption. Mulumba et al. proposed in [18] a methodology to

121 diagnose the presence of several faults affecting air dampers, cooling coil valve and return fan by

122 using a SVM in combination with an autoregressive model with exogenous inputs. Yan et al. proposed

123 in [19] a combination of two supervised techniques to diagnose the blockage of air dampers and coil

124 valve, the duct leakage and the return fan failure. In [19] a Classification Tree (CT) was developed,

125 which used in input both monitored data (i.e. air temperature and flow rate, fan speed and power, and

126 cooling coil valve position) and residuals obtained from a regression model of the fan speed, while

127 in output the labels of different faults were considered. The methodology developed in [19] made it

128 possible to accurately perform fault diagnosis, but without taking into account transient periods of

129 operation. Different classification models for fault detection were also compared in the work of

130 McHugh et al. [20] and the Classification (decision) Tree model was selected as the best choice for

131 the detection of steam or chilled water leakage.

132 The unsupervised methods proved to be particularly flexible for their nature in exploring data set

133 without any *a priori* constraint, as opposed to the supervised models [11].

134 Yu et al. proposed in [21] an unsupervised methodology to identify energy wastes and faults of a fan

135 in an AHU, by exploiting Association Rules Mining (ARM). This type of algorithm requires a strong

136 expertise by the analyst for the interpretation of the results, considering that the rule set extracted

137 could include also not-interesting information for the identification of anomalous operation of the air

138 conditioning system [21]. Many studies make use of ARM for the identification of faults in different

139 types of HVAC systems (e.g. district heating substation, AHU, chillers)[10]. ARM has been adopted

140 also for the analysis of a district heating substation in order to identify inefficient operation and sensor

141 faults by searching anomalous correlation expressed by association rules [22]. In order to help the

142 domain expert in the interpretation of the results, in [23] a methodology was proposed to reduce the

143 number of rules to be analysed and to effectively group them for distinguishing the faulty from the

144 normal operation. Furthermore, the temporal relation among the energy consumption of different

145 HVAC components was studied in [24] and [25] to determine the presence of faults and prevent a

146 reduction of energy performance over time.

147 A combination of a supervised and unsupervised methods (e.g., decision tree and clustering analysis)

148 was proposed in [26] and [27] for the detection of anomalous energy consumption in a group of smart

149   office buildings. Furthermore, Dey et al. achieved in [28] high values of accuracy in the automatic

150   FDD on fan coil units operation by combining MC-SVM and cluster analysis.

151   Du et al. in [29] proposed a methodology to identify faults of temperature, flow rate and pressure

152   sensors in a VAV system by implementing Artificial Neural Networks (ANNs) in combination with

153   a signal decomposition technique (i.e. Wavelet analysis). In [30], an ANN was combined with

154   clustering analysis to diagnose faults related to cooling coil valve, air damper and temperature sensors

155   in an AHU. In the first step, the ANN was used for the estimation of supply air and water temperature

156   to perform a residual analysis, then the methodology leveraged on clustering analysis for the fault

157   diagnosis stage. Guo et al. used a Hidden Markov Model (HMM) for the fault detection phase and a

158   cluster analysis for the identification of various types of faults such as the blockage of dampers, frozen

159   fan or unstable cooling coil valve control signal [31]. In [32] and [33], an unsupervised data-driven

160   approach was used to identify the presence of cooling coil valve blockage, heating coil valve leakage

161   and air damper blockage, by analysing the error generated from the reduction of variables by means

162   of Wavelet Transform and Principal Component Analysis. Successively, the fault diagnosis was

163   performed by analysing the trend of each variable during faulty conditions, in order to identify the

164   variable mostly influenced by the fault source.

165   Liang et al. in [34] proposed a methodology to diagnose the stuck of the recirculation damper and of

166   the cooling coil valve in an AHU, as well as the decreasing of the supply fan speed. In that work, an

167   SVM was used in combination with a white box model, exploiting the residuals obtained by

168   comparing actual and simulated fault-free values of supply and mixed air temperature, and cooling

169   coil outlet water temperature. Wu et al. in [35]combined a quantitative model-based method with an

170   unsupervised data-driven method to diagnose sensor faults, air damper blockage or frozen fan. In that

171   work, first the variables considered were reduced (i.e., by means of Principal Component Analysis),

172   then the presence of faults was investigated comparing actual monitored data with the estimation of

173   airflow rate and energy calculated by using simplified balance equations for energy and pressure-

174   flow. In other works, a qualitative-based approach was used to perform automatic FDD in

combination with the data-driven approach. In [36], the detection of faults occurring in an AHU was performed by exploiting "IF-THEN" expert rules related to the residuals of mixed air temperature, return air flow rate, supply air static pressure and cooling coil valve control signal, generated with different General Regression Neural Networks. In [37] the integration of expert rules with Bayesian Networks was pursued, in order to better isolate faults in AHU. Such approach made it possible to exploit the violation of expert rules, to better detect the co-occurrence of multiple faults at the same time.

The above reported literature review demonstrated how much the scientific research has been active in the field of artificial intelligence for FDD in AHU and HVAC systems. However, the opportunity to approach this well-known task (i.e., FDD) from this innovative point of view was mainly due to the growing availability of huge amount of monitored data, related to the actual performance of buildings and energy systems. In this context some projects, supported by the American Society of Heating, Refrigerating and Air- Conditioning Engineers (ASHRAE) made very comprehensive field surveys, laboratory tests and performance evaluations on the performance of HVAC systems also in faulty conditions. The outcomes of such projects (e.g., ASHRAE Project 1312-RP and 1043-RP) enabled a great spread of FDD methodologies which exploit experimental data.

Among the reviewed papers, several published studies focused on the ASHRAE RP-1312 data set for developing and testing FDD methodologies for AHUs [16,17,38–43]. Despite those papers discuss the results of FDD methodologies on the same data set, not always the assumptions behind the analysis are the same. The main differences are related to the operation mode considered (cooling, heating, spring), the number and the type of faults analysed, the regime of operation considered (transient, non-transient). However, from the analysis of these works, some general considerations can be made:

- In most of the cases the analysis is performed for the summer period achieving high values of accuracy in diagnosing faults (over 90% of accuracy),

- The analysis is performed for data collected with sampling frequency of 1-min (original granularity of the dataset),

- Data-driven models used for characterizing the normal behaviour of the AHU lack of interpretability (SVM, ANN)

- In most of the cases, the fault diagnosis is performed through interpretable classifiers (decision trees, Bayesian networks).

In this context, the present paper aims at introducing an FDD methodology for AHU systems (based on data of ASHRAE RP-1312) that is data-driven, fully interpretable and rule-based. Indeed, the rule-based approach can satisfy the user need of simplicity and interpretability while the data-driven nature of the methodology can enable the automatic learning of system operational patterns. Another objective is also to reduce the granularity of the dataset while maintaining good performance in fault diagnosis. In fact, analyse data with a high sampling frequency could expose the FDD tool to instabilities when deployed for operating in real time (presence of punctual anomalies, missing values, sensor network latency).

In the approach proposed in this paper two rule-extraction methods (association rule mining, decision tree) were employed for conducting FDD analysis in AHU system, by exploiting the reduction and transformation of multiple time series related to the operation variables of the system. In the next section a discussion is provided about the automatic extraction of rules in multiple time series (Section 210) and the work novelty is explained (Section 2.1); the case study analysed in the paper is presented in Section 3; a focus on data analysis methods exploited in the analysis is provided in Section 4 and a description of the proposed methodology is provided in Section 5. In Section 6, the results obtained from the application of the methodology are presented. Eventually in Section 7 the discussion of results and concluding remarks are provided.

2   Rule extraction in multiple time series for FDD in AHUs

The analysis reported in section 1.1 on the most relevant works published in the last few years, showed how FDD strategies in AHUs can widely benefit from the implementation of data mining and machine learning techniques, especially when they are supported by a robust expertise in building physics for an effective exploitation and interpretation of the extracted knowledge. However, the complexity of an AHU with multiple operational parameters and the temporal interactions among them makes the effective characterisation of its behaviour challenging.

The operation of an AHU system is characterized by two major time-regimes, namely transient and non-transient. The transient operation typically occurs when the AHU is started-up and is approaching the steady state conditions, or when it is shutdown or disturbed from its non-transient regime. The disturbances could be caused by either variation of thermal loads or by feedback controls. During transient periods some variables can exhibit strong variation in short time and a significant temporally lagged response with respect to the control signals. In addition, the behaviour of an AHU system varies as its mode of operation changes during the day and the year i.e., off mode, heating mode, free cooling mode, and cooling mode. Therefore, a robust data-driven-based FDD tool should be able to automatically determine the mode of operation of the system, to prevent false alarms from being generated. For example, normal behaviour during summer season may be faulty if the system is operating in heating mode (winter season). In order to avoid that condition, FDD tools in AHU systems are characterized by a hierarchical architecture that makes it possible to exploit only the portion of knowledge that is consistent with the specific operation mode considered. In this perspective, when using data-driven based FDD tools it is necessary for the training data to be exhaustive as possible for each operation mode.

However, given their complexity, data-driven-based FDD tools often lack in interpretability. In this context, the use of rule-based data-driven methods for FDD can satisfy the user need of simplicity in terms of understanding the FDD tool, using, commissioning and integrating it with existing BAS, and updating it. For this reason, great attention has been paid in this study to the application of advanced

249 supervised and unsupervised rule extraction methods (i.e., decision trees, association rule mining)

250 with reference to multivariate problems.

251 The operation of an AHU is a perfect case that can be effectively described through the analysis of

252 multiple time series (defined as series data points indexed in time order) associated to each operational

253 variable of the system. However, the large number of time series with high sampling frequency could

254 significantly increase the complexity and computational cost of the analysis, often making necessary

255 a proper reduction (aggregation in the time domain) and discretization (quantization of the signal

256 value) of data. This is a challenging task, considering that each variable has its own behaviour and

257 distribution and, as a consequence, the optimal time aggregation and value discretization of the signal

258 need to be identified with the aim of minimizing the information loss and of maximizing the mining

259 performance. Such preparation of the time series is an essential step in FDD methodologies based on

260 rule extraction techniques (e.g., based on association-rule mining algorithms or decision trees) that,

261 in the literature, have been used for effectively mining co-occurrences or implications between

262 discrete values and events in the time domain during HVAC operation [19,24,44].
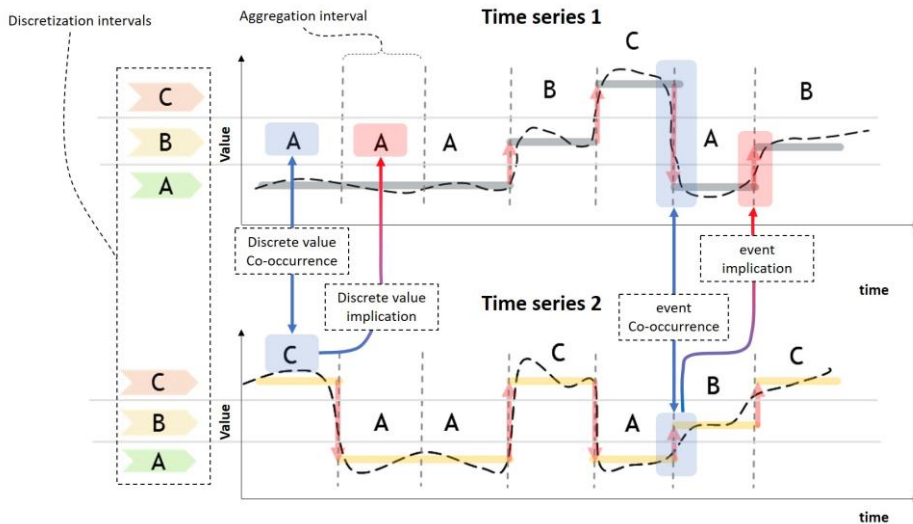
263

264 *Figure 1. Graphical representation of co-occurrence and implication between discrete values and events among*

265 *multiple time series.*

266 Figure 1 depicts in graphical form the concepts, of discrete value, event (change of discrete value

267 between two contiguous aggregation intervals), co-occurrence and implication of discrete values and

268   events with reference to two time series encoded in symbols by means of Symbolic Aggregate

269   approXimation (SAX) [45].

270   When multiple time series are considered, rule extraction techniques can be categorized in intra-

271   transactional and inter-transactional respectively. The first type of extraction aims at discovering co-

272   occurrences between discrete values and events that frequently happen at the same time among

273   different time series (Figure 1). The second type of rule extraction is more complex, considering that

274   the occurrences of discrete values and events among different time series, in that case, are searched

275   taking into account the existence of a time lag (Figure 1). During transient periods of AHUs operation,

276   the latter approach is particularly favourable in describing phenomena that are characterized by

277   temporal dependences among variables representative of the system operation (e.g., change of status

278   in a fan speed and the corresponding effect on supply air temperature).

279   In order to develop an FDD process capable to be flexible in relation to different conditions of

280   operation in AHUs, the present study proposes the application of two rule extraction methodologies

281   tailored for both transient and non-transient periods.

282   The developed framework aims at preventing anomalous running modes of AHUs, which could lead

283   to significant energy waste over time and/or discomfort conditions in the built environment.

284   The analysis relies on temporal abstraction as a pre-processing stage. Temporal abstraction is aimed

285   at reducing and transforming time series in discrete-time and discrete-value signals through

286   aggregation on the time axis and discretization of the value in order to perform the extraction of

287   interesting co-occurrences and implications. In this study, an adaptive process based on a Symbolic

288   SAX is employed for conducting the temporal abstraction.

289   Furthermore, strong relations between events (i.e., change of discrete value between contiguous

290   aggregation intervals) are automatically mined by means of temporal IF-THEN association rules in

291   the transient period of AHU operation (i.e., start-up phase), considering an intra-transactional

292   approach for characterizing the fault-free behaviour of the system. Similarly, during the non-transient

293   period of operation, a set of classification trees are developed for extracting reference patterns in the

294   form of decision rules. Potential faulty conditions are then detected when the discovered association

295   and decision rules are violated over time. Successively, the identified anomalous patterns (during the

296   non-transient period) are exploited for performing a diagnosis of the most probable faults associated

297   to a specific kind of rule violation by means of a classification algorithm.

2.1   Novelty of the paper

299   The present work introduces an automatic methodology for performing an FDD analysis in AHUs by

300   using experimental data obtained in the framework of the ASHRAE project RP-1312. The entire

301   process relies on the application of data mining-based algorithms in order to develop a tool capable

302   to detect and diagnose operational faults in AHUs which can determine energy waste over time and

303   the occurrence of discomfort conditions in the built environment.

304   Based on the FDD literature review presented in section 1.1, the main innovative aspects introduced

305   by the present paper are the following:

306   - An adaptive process of data reduction and transformation is employed to develop a robust

307   FDD methodology. In complex systems as AHUs, the number of monitored variables and

308   their sampling frequencies could be very high. Extracting only key information from large

309   data set is essential for reducing redundancy, complexity and computational cost. In this study,

310   the methodology makes it possible to achieve good performance in FDD (comparable to other

311   studies focused on the same dataset [16,17,38–43]) leveraging only on the analysis of

312   significant discrete intervals of the operational variables over time.

313   - The start-up period of AHU operation is isolated and treated separately by developing a

314   tailored analytics module (instead of being filtered out as happened in other studies focused

315   on the same dataset [16,17,38–43]). During transient period of operation time lags occur for

316   example between a change of status in the fan speed and the corresponding effect on supply

air temperature. For this reason, temporal association rules are extracted, following an intra-transactional approach, for discovering associations between events during transient periods, across multiple time series, that frequently occurs within a time lag.

- The characterization of normal behaviour during the non-transient period is completely automated and performed by using a set of estimation models based on decision trees. In comparison to other studies focused on the same dataset [16,17,38–43], the reference behaviour of the AHU is evaluated estimating the most probable discrete value of each influencing operational variable in relation to all the others monitored. In that way, all the existing relations between variables are exploited through several estimation models, for detecting potential faulty conditions. Such approach exhibits high flexibility and generalizability in the formulation of the FDD problem.

- A fault diagnosis during non-transient period of AHU operation is performed by employing a decision tree, capable to extract rules for the classification of typical faults. The diagnosis process exploits the residuals evaluated by means of a set of estimation models as input attributes for the classification of the most probable faults.

In that perspective, this study was aimed at conceiving, developing and testing a methodological framework that introduces the aforementioned novelties in automatic FDD, in as robust a way as possible. As previously stated in the literature review, several studies considered the RP-1312 data set in the analysis, achieving an accuracy in fault diagnosing over 90%. As a consequence, the main objective of this study is not to improve the (already high) FDD performance achieved on the RP-1312 dataset, but rather to demonstrate the opportunity to achieve high performance as well through a fully interpretable and simplified data-driven approach, based on rule extraction techniques.

3 Case study

In order to test the validity and the effectiveness of the proposed methodology, operational data related to two AHUs collected in the framework of the Research Project ASHRAE RP-1312 [14]

342   were analysed. The system investigated is a Variable Air Volume (VAV) AHU. A VAV system is

343   able to modulate the air flow rate according to the variation of the building load and it is typically

344   made up of 4 subsystem controllers, acting on supply air temperature, dampers and valves, supply air

345   static pressure and return air flow rate. Specifically, the control logic maintains the supply air

346   temperature set-point acting on damper and valve positions, according to the mode of operation (i.e.

347   heating, cooling with partial mixing of outdoor air, cooling with 100% of outdoor air, cooling with

348   minimum outdoor air).

349   Furthermore, also the static pressure of the supplied air and the difference between the supply and

350   return air flow rate is controlled. The return air flow rate is modulated acting on the mixing dampers

351   and the return fan speed, while the system maintains the static pressure set point for the supply air.

352   As a result, the difference between the supply and return air flow rate is kept constant [12].

353   The dataset used in this paper is particularly interesting as it includes several running conditions for

354   two AHUs in faulty and fault-free operation. The faulty operation was obtained by artificially

355   implementing a number of different faults. The site, where the monitoring data have been collected,

356   is a test facility simulating a typical schedule of occupancy in commercial building.
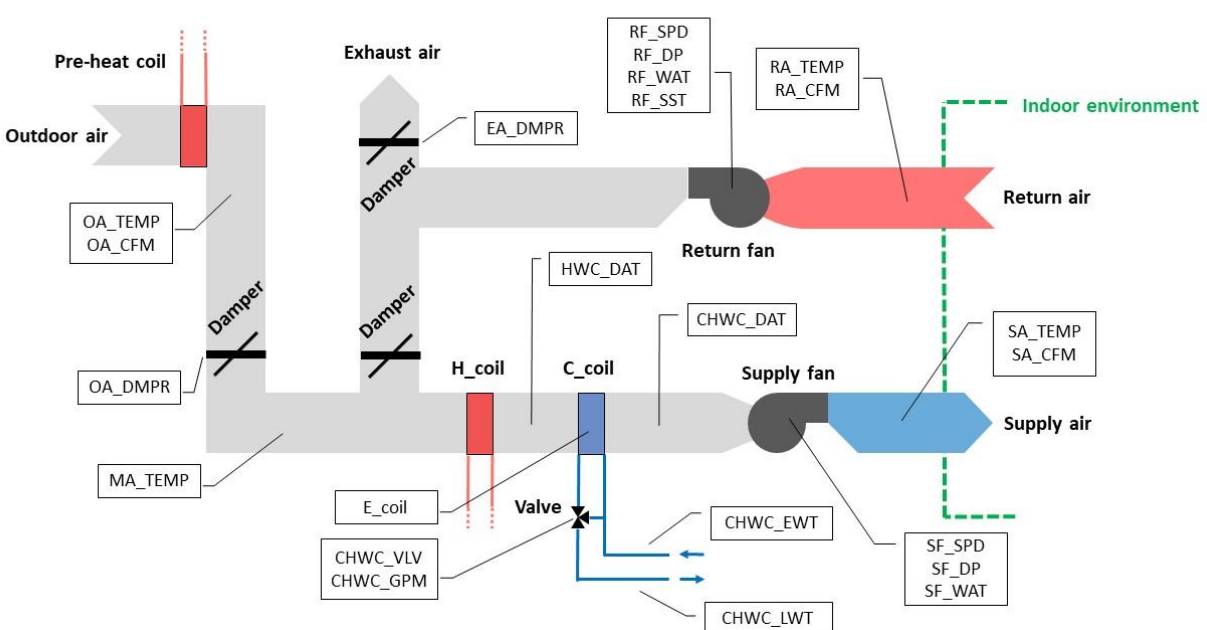
357

358   *Figure 2. Scheme of the AHU analysed (refer to Table 2 for variable encoding).*

359 The monitoring data were gathered from two AHUs of the facility (AHU-A and B), which are

360 perfectly identical from technical and operational points of view and serve specular zones. The zones

361 served by AHU-A and B face east and west orientation, respectively, in order to be comparable also

362 under the aspect of the thermal loads. The AHUs are characterised by a mixing chamber, to mix return

363 air with outdoor air by means of dampers. Each AHU is equipped with heating and cooling coils and

364 VAV devices to locally adjust the supply air temperature. However, the control volume considered

365 in this work excludes the local VAV devices.

366 Figure 2 shows a schematic configuration of the system with the indication of the monitored variables

367 (a description of the variables is provided in Table 2).

368 In the context of the ASHARE project, a number of different faults were implemented one per time,

369 each for a whole day, only in the AHU-A, in order to analyse independently the effects of each fault.

370 The AHU-B was always run in fault-free conditions to have a reference of the normal operation. The

371 data collection was conducted over three seasons and only the monitoring data of the summer season

372 were considered in this study.

373   *Table 1. Tags and descriptions of faults.*

Fault Tag	Description	Number of days
CCVS15	Cooling coil valve stuck at 15%	1
CCVS65	Cooling coil valve stuck at 65%	1
CCVSFC	Cooling coil valve stuck fully closed	1
CCVSFO	Cooling coil valve stuck open	1
EASFC	Exhaust air damper stuck fully closed	1
EASFO	Exhaust air damper stuck fully open	1
Normal	Normal operation	22
OAS45	Outdoor air damper stuck 45%	1
OAS55	Outdoor air damper stuck 55%	1
OASFC	Outdoor air damper stuck fully closed	1
RFCF	Return fan complete failure	1
RFF30	Return fan at fixed speed (30%)	1

374

375 The dataset consists of multiple time series (one for each monitored variable) with a length of 33 days

376 and a sampling time of 1 minute. In particular, 22 out of 33 days are tagged as fault-free days while

377 the remaining 11 days correspond to different faulty conditions. Table 1 summarizes the number of

378 fault-free and faulty days, the description of each fault and the tags used for labelling each day

379 included in the monitoring campaign.

380 A feature selection was preliminarily performed on the basis of expert considerations to focus the

381 analysis only on relevant variables.

382 As a result, the variables considered for the implementation of the FDD methodology are: the

383 electrical load, the pressure drop and speed of fans, the flow rate and temperature of the air measured

384 in different parts of the system, the damper position, the valve position, the water flow rate and energy

385 transferred in the cooling coil.

386 Table 2 reports the list of the 23 variables considered for the analysis, together with the specification

387 of labels, description, ID number and unit of measurement for each variable.

388 *Table 2. List of variables considered in the analysis.*

Variable	Description	ID n°	Unit
SF_WAT	Supply fan power	1	W
RF_WAT	Return fan power	2	W
SA_CFM	Supply air flow rate	3	m^3/h
RA_CFM	Return air flow rate	4	m^3/h
OA_CFM	Outdoor air flow rate	5	m^3/h
SA_TEMP	Supply air temperature	6	°C
MA_TEMP	Mixed air temperature	7	°C
RA_TEMP	Return air temperature	8	°C
HWC_DAT	Heating coil air temperature	9	°C
CHWC_DAT	Cooling coil air temperature	10	°C
SF_DP	Supply fan pressure drop	11	Pa
RF_DP	Return fan pressure drop	12	Pa
SF_SPD	Supply fan speed	13	%
RF_SPD	Return fan speed	14	%
OA_TEMP	Outdoor air temperature	15	°C
CHWC_EWT	Cooling coil input water temperature	16	°C
CHWC_LWT	Cooling coil output water temperature	17	°C
CHWC_GPM	Cooling coil water flow rate	18	m^3/h
E_ccoil	Cooling coil power	19	kW
CHWC_VLV	Cooling coil valve position	20	%
EA_DMPR	Exhaust air damper position	21	%
OA_DMPR	Outdoor air damper position	22	%
RF_SST	Return fan start/stop signal	23	-

389

390 For the application of the proposed methodology, the data sample was split into two datasets. The

391 first one was used for the characterization of the normal operating condition of the system, while the

392 latter was used for the fault detection and diagnosis. The first dataset is composed of 20 days tagged

393 as "Normal" (training dataset), while the second by the rest of the days including 2 "Normal" days

394 and 11 "Faulty" days (testing dataset).

4 Description of the data analysis methods

396 In this section, the overview is presented of the techniques used for the proposed FDD methodology,

397 describing their main features in relation to the FDD problem under investigation.

4.1 Adaptive symbolic aggregate approximation

399 The Symbolic Aggregate approXimation (SAX) is a temporal abstraction technique capable to reduce

400 the dimension of a time series of length n in a time series of length m with m < n, and to transform it

401 in a symbolic string. The reduction of the time series is performed through a Piecewise Aggregate

402 Approximation (PAA), which segments the time axis in equally sized non-overlapping time windows

403 (i.e., aggregation intervals). The PAA approximates the original time series replacing the values

404 within the same aggregation interval with their mean value.

405 The transformation of the time series is then performed by substituting the values of the PAA with

406 symbols. To this purpose, the y-axis is discretized in a pre-defined number of regions and a symbol

407 is associated to each of them. Lin et al. in [46] proposed a simple procedure to perform the SAX,

408 employing a Z-score transformation (i.e., $Z(t) = \frac{x(t) - \mu}{\sigma}$ where μ is the mean value of the sample

409 and σ the standard deviation) before the data reduction and identifying the desired range of each

410 symbol assuming a-priori a Gaussian distribution of data.

411 A variation of SAX technique, called adaptive Symbolic Aggregate approXimation (aSAX), was

412 proposed in the literature [45]in order to improve the quality of the discretization in the case of non-

413 normal distribution of data. The adaptive symbolic aggregate approximation introduced by Pham et

414   al. [45] is based on the original SAX method, but an adaptive process is used for the identification of

415   breakpoints (i.e. the position of boundaries of each symbol range). The position of the adaptive

416   breakpoints is evaluated through a univariate clustering procedure, that minimises the total

417   representation error after the SAX transformation.

418   In this paper, the aSAX algorithm has been employed to improve the results of the automated and

419   unsupervised discretization process, which represents the most important analysis for ensuring the

420   robustness of the "event" extraction from time series.

421   ## 4.2   Temporal Association Rules Mining

422   Association Rule Mining (ARM) is an unsupervised data mining method for identifying all

423   associations and correlations between attribute values in a set of categorical/discretized data [47]. The

424   output is a set of association rules that are used to represent patterns of attributes that are frequently

425   associated together (i.e., frequent patterns).

426   Let $I = \{i_1,\ i_2, \dots i_d\}$ be the set of all items in a dataset and $D = \{d_1,\ d_2, \dots d_d\}$ be the set of all

427   transactions. Each transaction d_i contains a subset of items chosen from I. In association analysis, a

428   collection of items is named *itemset* and the transaction width is defined as the number of items

429   present in a transaction. A transaction d_j contains an itemset X if X is a subset of d_j. An important

430   property of an itemset is its support count, that corresponds to the number of transactions that contain

431   a specific itemset. The support count, σ(X), for an itemset X can be expressed as follows [47] (eq.1)

432    $$\sigma(X) = |\{d_i | X \subseteq d_i, d_i \in D\}| \qquad (1)$$

433   Association rules are usually represented in the form X → Y, where X (also called antecedent) and

434   Y (also called consequent) are disjoint item sets (i.e., $X \cap Y = \emptyset$). Rule quality is usually measured

435   through rule support and confidence. Rule support is the fraction of the total number of transactions

436   in which both the item sets X and Y occur while confidence determines how frequently items in Y

437   appear in transactions that contain X. According to [47], Support $s(X{\rightarrow}Y)$ and Confidence $c(X{\rightarrow}Y)$

438   can be calculated with the following equations (eq. 2 and 3):

439

$$\text{Support}, s(X \rightarrow Y) = \frac{\sigma(X \cup Y)}{N} \tag{2}$$

440

$$\text{Confidence}, c(X \rightarrow Y) = \frac{\sigma(X \cup Y)}{\sigma(X)} \tag{3}$$

441   where N is the total number of transactions. Therefore, given a dataset D, the generic record of which

442   is a set of items, an ARM process discovers all association rules with support and confidence greater

443   than, or equal to, minimum thresholds defined a-priori by the analyst (i.e, MinSup and MinConf).

444   In the context of discrete-value-transactions, association rules can be used as an efficient method for

445   mining co-occurrences or implications also between events in the time domain (Temporal Association

446   Rule Mining (TARM)). TARM is an extension of sequential pattern mining, which is an important

447   data mining method with broad applications, capable to extract frequent itemset sequences while

448   maintaining their order. Many sequential pattern mining algorithms, such as GSP [48], PrefixSpan

449   [49,50], SPADE [51], and SPAM [52], have been proposed. However, those sequential pattern mining

450   algorithms consider only the itemset occurrence order, but do not consider the time intervals between

451   successive item sets (temporal constraint of event association). To that purpose, in the literature

452   several sequential pattern mining algorithms were proposed, to deal with the extraction of sequential

453   patterns considering the existence of interval between item sets (in terms of item gap and time

454   interval) [53–56]. Such algorithms extract rules, satisfying not only user-specified minimum support

455   constraints, but also user-specified gap constraints. The minimum and maximum gap values should

456   be defined as constraints by the user. For those rules, the search space in the time domain is

457   represented by a sliding window, the length of which is set in advance by the analyst. In detail, this

458   kind of rules can be represented in the following form: $X \xrightarrow{t} Y$. Therefore, the occurrence of the

459   antecedent itemset X implies the occurrence of the consequent itemset Y within a time t.

460   In this paper, the extraction of temporal association rules is performed by means of the cSpade,

461   algorithm based on [51]. The algorithm was implemented in R [69], including the rule extraction

462   phase which was performed by using the "cSpade" function of the "arules" package [70].

463   That algorithm extracts sequential rules, considering some constraints defined by the user according

464   to his/her needs. The constraints may drive the mining of frequent patterns from the database of

465   transactions, for instance by setting the length of the sliding window, or a minimum time gap between

466   antecedent and consequent of the rules.

467   However, since the database of transactions considered in the present study is generated by using a

468   sample-by-sample sliding window approach, the number of the transactions N results to be very high

469   with items mostly overlapped. For this reason, the calculation of rule support $s(X{\rightarrow}Y)$ cannot be

470   performed with the canonical formulation. In fact, the value of support $s(X{\rightarrow}Y)$ calculated according

471   to eq. 2 can be affected by the high value of the denominator (i.e., the total number of transactions),

472   suggesting the use of a formulation less sensitive to the sample size [57].

473   In this study, according to [58], the support of an association rule is defined as the ratio between the

474   number of transactions that include both antecedent and consequent, and the number of transactions

475   that include at least the consequent itemset (eq. 4).

$$\text{Support}, s(X \rightarrow Y) = \frac{\sigma(X \cup Y)}{\sigma(Y)} \qquad (4)$$

476

477   The support calculated with eq. 4 has the denominator dramatically lowered in comparison to the one

478   in eq. 2 and makes it possible to have high values of support also for large transaction datasets,

479   obtained through a sliding window. The support calculated through Eq. (4) assesses the frequency of

480    $X \cup Y$ on a smaller portion of the total number of transactions (i.e., only the transactions that include

481   the consequent itemset Y). The support is in the range (0-1) and allows an easier extraction of rules

482   to be assumed as reference patterns (i.e., with high support) of the occurrence of a specific condition

483   over time (i.e., consequent itemset Y). However, the confidence can be still calculated according to

484   Eq. (3) only if the consequent itemset Y occurs in a transaction not violating the chronological order

485   respect to the antecedent itemset X.

486   In general, the mining of association rules can be summed up as a two-step's procedure. In a first

487   phase, the frequent itemset with a support greater than the MinSup are extracted, then the confidence

488   is considered for filtering out rules that consist in weak implications [59]. In this paper, the same two-

489   steps procedure is followed but additional metrics are also considered in the rule filtering phase (as

490   discussed in section 5.3).

491   ## 4.3   Classification And Regression Tree

492   Decision trees are machine-learning algorithms that are used to develop descriptive and/or predictive

493   models from a collection of records. Each record can be expressed as a tuple (**x**,y), where **x** represents

494   the explanatory attribute set while y is the target attribute. The type of target attribute is the key factor

495   that distinguishes classification from regression trees (i.e. discrete attribute in the first case and

496   continuous attribute in the second one) [47]. In this work, the Classification And Regression Tree

497   (CART) algorithm, based on recursive partitioning algorithm [60], has been selected to conduct a

498   predictive modelling task, as it is able to easily handle categorical attributes as both explanatory and

499   target attributes. The CART is a specific machine learning technique that is based on a recursive

500   binary splitting of the whole feature space into finite disjoint sets, and its output can be translated into

501   a hierarchical tree structure composed by nodes and directed edges (i.e., branches). The leaves (i.e.,

502   final nodes) represent the predicted class labels of the target attribute, while the branches represent

503   the conjunctions of the explanatory attributes that lead to the class labels

504   The development of a classification tree unfolds over two steps: training and testing of the model.

505   Each decision tree developed has been pruned following a cost-complexity approach and validated

506   through a k-fold cross validation process as explained in [61]. The development of a classification

507   tree unfolds over two steps: *training* and *testing* of the model. Firstly, all the records are grouped in

508   the root node and the CT algorithm iteratively evaluates the best partitioning of the dataset, using the

509   explanatory attribute that minimises the average impurity measure (e.g., Gini index, Entropy) of the

510   child nodes after each split. If no stopping rules are set by the analyst, the classification tree grows

511   continuously until the impurity in the leaf nodes of the target variable is zero. In order to avoid this

512   condition of model overfitting, various types of appropriate early stopping criteria can be set in

513   advance by the analyst (e.g., minimum number of cases in parent and child nodes, maximum tree

514   depth, minimum reduction in node impurity after splitting). Even when the early stop criteria have

515   been satisfied, the tree may continue to be quite large and/or complex completely losing its

516   interpretability. For this purpose, it is possible to define a cost-complexity parameter (cp) during the

517   model validation phase, for optimising the trade-off between the cost of misclassification and the tree

518   complexity. Therefore, the cp allows the analyst to set the right tree size by pruning branches and leaf

519   nodes that do not significantly increase the model performance.

520   Starting from the fully grown tree, the cost-complexity pruning procedure is repeated iteratively, and

521   smaller and smaller subtrees are found until the root node is reached. At the end of the iterations, the

522   final pruned tree can be evaluated by plotting the relative errors of the subtrees versus their cp values.

523   This kind of plot usually shows an initial sharp drop, followed by a relatively flat region. When the

524   decision tree is subject to a validation procedure (e.g., k-fold cross-validation), it is also possible to

525   compute a standard error for each relative error of the sub-tree. The choice of the best subtree starts

526   from the flat region of the subtree errors that includes the minimum cross validated error that has

527   been achieved. In fact, the values falling within one standard error of the achieved minimum risk (i.e.,

528   1-SE rule) identify statistically equivalent sub-trees [60]. The simplest model (with the minimum

529   number of final nodes) of all the identified sub-trees in the flat region is then chosen.

530   K-fold cross-validation has been used in this paper. For this kind of method, the original sample

531   of data with M objects is divided into k equal sized subsamples. A single subsample is selected for

532   the evaluated k subsamples as a validation dataset for testing the model, and the remaining ($k-1$)

533   subsamples are used for the training. This process is then repeated k times, using a subsample at a

534   time for the testing

535   In this paper, all the classification trees developed for extracting decision rules have been subjected

536   to the previously described procedure of validation and pruning (as discussed in section 5.4).

537   ## 5   Methodological framework of analysis

538   The methodology relies on the application of both supervised and unsupervised algorithms to perform

539   robust fault detection and diagnosis in AHUs.

540   The framework unfolds over different stages as shown in Figure 3. Two different analytics modules

541   are proposed for developing an FDD tool tailored for both transient and non-transient conditions of

542   the AHUs operation. For that purpose, in the methodological framework, a data segmentation phase

543   is preliminarily carried out in order to split the data according to the regime of operation they belong

544   to (i.e. transient or non-transient). In the following sections the pre-processing analysis, applied to the

545   entire dataset, and the two analytics modules, tailored for transient and non-transient periods,

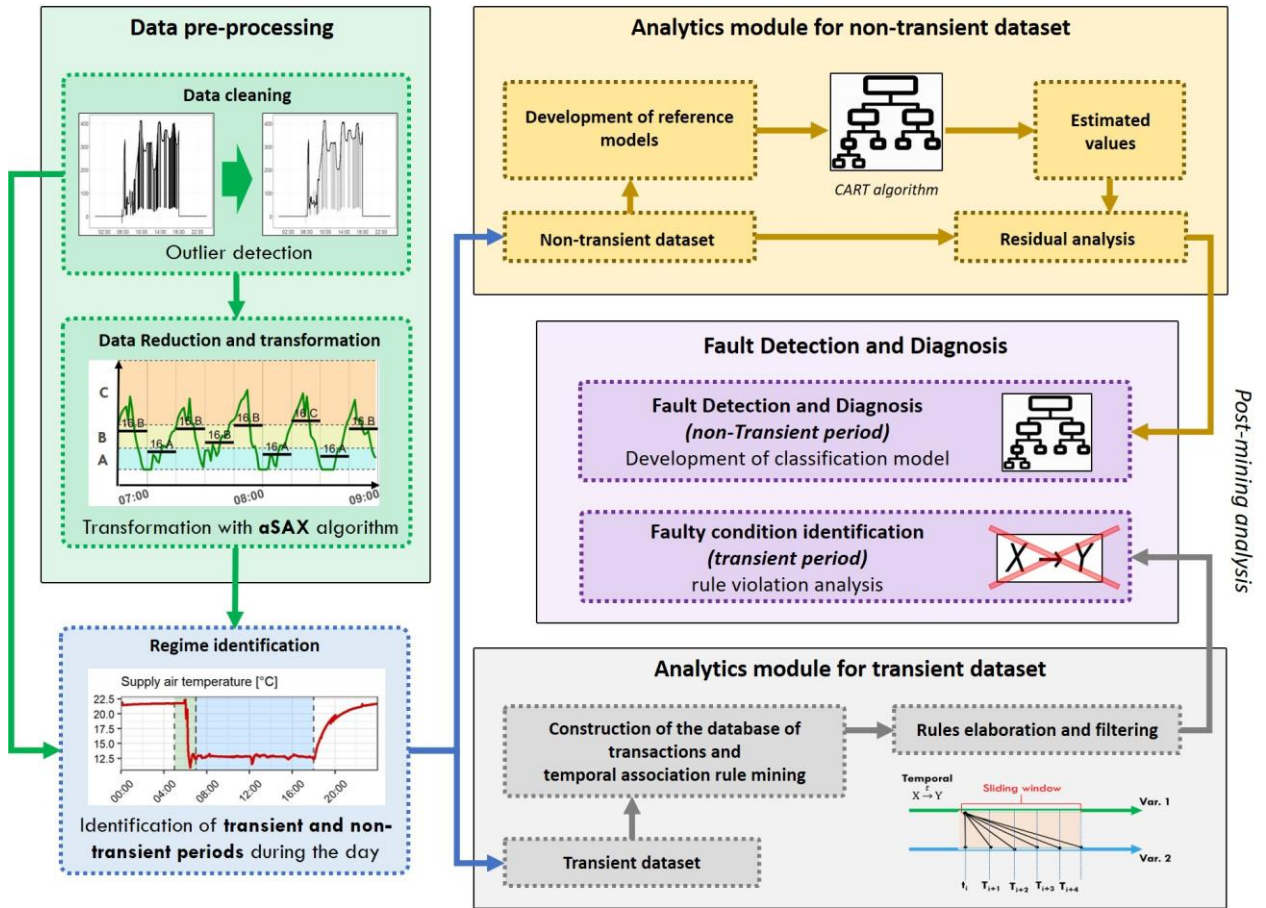546   respectively, are then described.

Figure 3. General framework of the analysis.

5.1 Data pre-processing stage

550 The pre-processing stage consists of three main tasks i.e., cleaning, reduction and transformation,

551 typically accomplished for preparing the data sets. In detail, outlier detection and replacement are

552 firstly performed (for each time series) by using the Hampel filter method [62]. For each data point

553 in the time series, the algorithm computes the median of a window that includes the considered data

554 point and its k surrounding samples. If a data point differs from the median by more than a standard

555 deviation, it is tagged as a statistical outlier and replaced with the median.

556 The monitoring data were available in time-series with a sampling time of 1-minute, which would

557 make the analysis onerous to be performed. For this reason, in a successive step a data reduction and

558 transformation process is performed by means of the adaptive Symbolic Aggregate Approximation

559 (aSAX) method [45]. This algorithm is employed for reducing the time series through a piecewise

560 technique aggregating data with a fixed length window from 1 minute to 15 minutes and then for

561 transforming it into a symbolic string. The objective is to maximise data compression and minimise

562 the complexity of the time series while preserving important information. The symbolic

563 representation of time series is always subjected to information loss due to the piecewise aggregate

564 approximation (especially information about the slope). However, when the segments are encoded in

565 symbols it is possible to preserve qualitative information about global trends of the time series, and

566 to easily detect important changes of patterns over time.

567 Figure 4 reports an example of data reduction and transformation through aSAX algorithm for a

568 portion of the time series related to the variable encoded with the ID n° 16 according to Table 2 (i.e.,

569 *cooling coil input water temperature* (CHWC_EWT)). The figure shows the time series after the

570 application of the Hampel filter (green curve) and the time series in form of constant approximated

571 piecewise (black lines). Furthermore, Figure 4 also shows the result of the aSAX transformation of

572 the time series into a symbolic string. The variable can assume three discrete values encoded with the

573 symbols 16.A, 16.B or 16.C according to the region the piecewise segments of 15-min fall in.
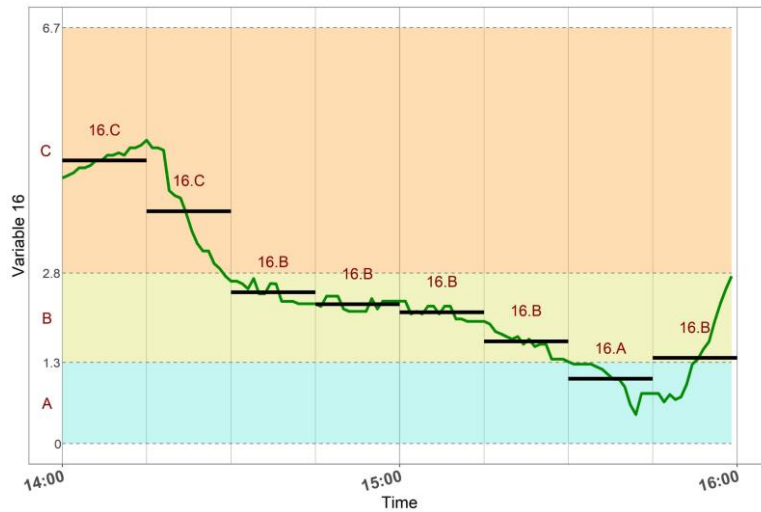
574

575 *Figure 4. Example of aSAX transformation for a numerical variable.*

576 The obtained symbol sequence is 16.C-16.C-16.B-16.B-16.B-16.B-16.A-16.B from which it is

577 possible to infer that the original time series is characterized by changes in the pattern at times 14:30,

578 15:30, 15:45, that in this work are intended as events.

579   As a result, time series are transformed in discrete-time discrete-value sequences of equidistant

580   symbols making it possible to extract events from them.

581   ## 5.2   Regime identification

582   At this stage, a regime identification is performed on a daily scale, to detect when transient and non-

583   transient conditions typically occur during the AHU operation.

584   To that purpose, an automatic regime detector is used to identify the transient period and separate it

585   from the non-transient one. The details of the detector used are the same as that reported in [16][63].

586   The transient identification is performed on data with sampling time of 1 minute, specifically

587   analysing the *cooling coil valve position* (CHWC_VLV), the *supply air temperature* (SA_TEMP),

588   *supply fan speed* (SF_SPD) and the supply air static pressure. Then, the frequency of transient data

589   points during the day is evaluated for each 15-min aggregation interval, derived from the data

590   reduction phase (Figure 5).   Thanks to that analysis, it is possible to establish during which

591   aggregation interval, out of the reduced (15-min-long) daily time series, a transient condition has the

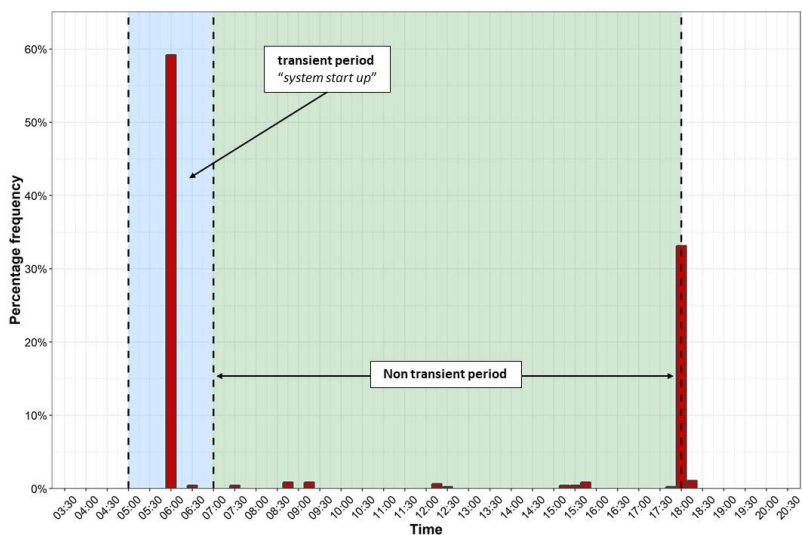592   highest frequency of occurrence.

593

594   *Figure 5. Identification of the transient period.*

595   Starting from such aggregation interval of 15 min, the transient period is evaluated considering a time

596   window of two hours (i.e., blue area of the plot) that includes one hour before and later the aggregation

597   interval considered (Figure 5).

598   As can be noticed from Figure 5, transients occur at the start-up and the shut-down of the AHU.

599   Among the two transient periods, only the start-up transient is investigated in this paper because

600   during that period the system dynamics affects the successive operation, while in the other case the

601   system is thereafter turned off.

602   As a result, the non-transient period is supposed to start at the end of the start-up time interval and to

603   end when the system is turned off.

604   Therefore, excluding the night hours, during which the AHU is certainly not operated, the dataset is

605   segmented as follows:

606   • From 05:00 to 07:00: transient period labelled as "*system start-up*";

607   • From 07:00 to 18:00: non-transient period.

608   In the following sections a tailored FDD methodology for each operation regime of the systems under

609   analysis (i.e., transient, non-transient) is presented.

610   ## 5.3 FDD methodology for the transient period

611   The main flow of FDD research reported in literature has been carried out in a steady-state approach

612   [14,17,19,64,65], because the operating characteristics during this operation is relatively more

613   credible and reproducible than in a transient state [64].

614   Transient data are characterised by great variation in the time domain and require specific data

615   analytics algorithms to be employed to properly reflect the system dynamics. The herein proposed

616   methodology provides, as a main added value to what was already present in literature papers, a

617   tailored approach for such condition of operation.

618 An overall procedure is developed to obtain temporal association rules that are representative of

619 frequent relationships between events in multiple time series, using a time window and a time lag.

620 As discussed in Section 4.2 temporal association rules are an interesting extension of association rules

621 that include a temporal constraint, which leads to different forms of IF-THEN implication over time.

622 When an event leads to the occurrence of another event, there may be causal relationship or certain

623 correlation between them. The corresponding mining purpose is to find out the reference fault-free

624 association rules between events and time in a temporal transaction dataset, whose violation can

625 suggest the presence of faulty conditions during the start-up period of the AHU system. The extraction

626 makes it possible to find those sequences of events that appear many times among monitored fault-

627 free days and have a high rate of occurrence (i.e., reference rules).

628 The reference association rules have been searched in the 20 days tagged as fault-free (training

629 dataset) while the remaining 2 fault-free days and 11 faulty days (testing dataset) were used in the
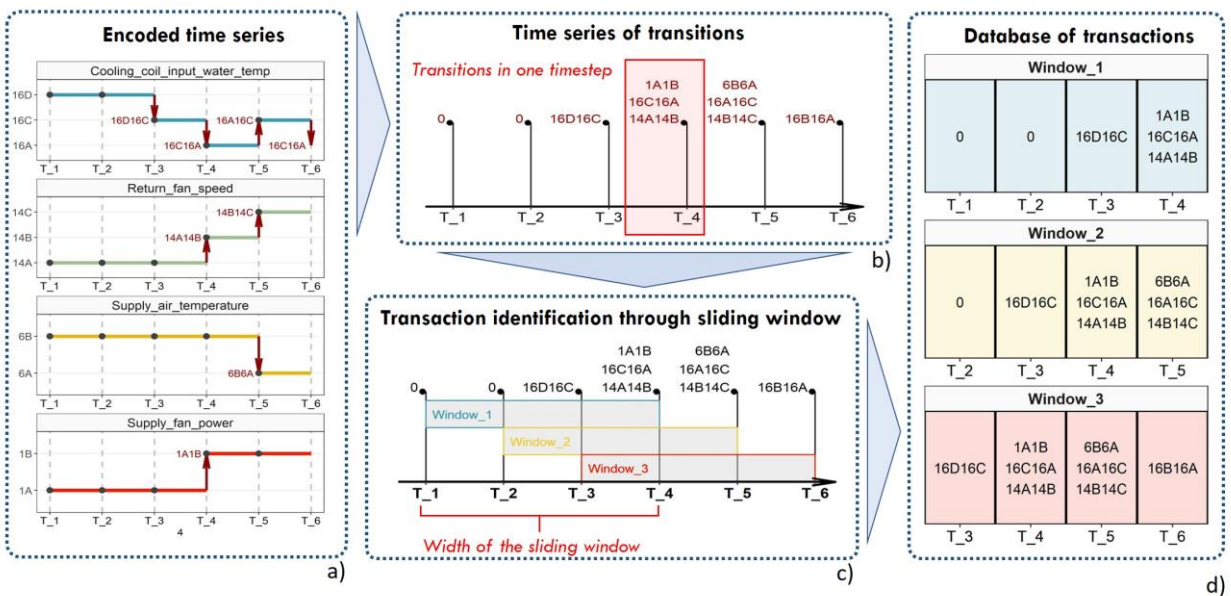
630 successive fault detection phase.

631

632 *Figure 6. Procedure for the construction of the database of transactions.*

633 Before extracting reference temporal association rules from data, it is necessary to create the database

634 of transactions T following the framework shown in Figure 6.

635 The first step consists of putting together all the transitions that occur in each time series into a unique

636 multivariate time series of transitions.

637 In particular, according to the symbolic transformation performed during the pre-processing stage a

638 transition in a time series is a kind of event that corresponds to the change of symbol (i.e., encoded

639 discrete values of the variable) in a specific timestep across two consecutive aggregation intervals.

640 As an example, Figure 6 (a) shows six timesteps of four time series (i.e., *cooling coil input water*

641 *temperature* (CHWC_EWT), *return fan speed* (RF_SPD), *supply air temperature* (SA_TEMP), *supply*

642 *fan power* (SF_WAT)). The time series *supply fan power* (SF_WAT) corresponds to the operation

643 variable of the AHU encoded with the ID n° 1 and assumes only two discrete values (encoded with

644 the symbols 1A and 1B) along the six timesteps considered. In the same way the time series *return*

645 *fan speed* that corresponds to the operation variable of the AHU encoded with the ID n ° 14, assumes

646 three discrete values (encoded with the symbols 14A, 14B and 14C) among the six timesteps. If two

647 consecutives aggregation intervals are encoded with the same symbol, no transition (i.e., event) is

648 detected. Otherwise, during a specific timestep, a transition (i.e., event) is encoded reporting the ID

649 n° of the variable and the two symbols included in the change of discrete value. For example,

650 according to Figure 6 (a), at the first timestep T_1 for any time series, a transition does not occur and

651 then 0 is stored in the time series of transitions (Figure 5 (b)). On the contrary, at the fourth timestep

652 T_4, a transition occurs for the time series 1, 14 and 16. In particular, for time series 1 and 14, occurs

653 a change from symbol "A" to symbol "B" (events encoded as "1A1B" and "14A14B" respectively)

654 while for time series 16 the variable changes symbol from "C" to "A" (event encoded as "16C16A").

655 Once the encoded events are stored in the multivariate time series of transitions (Figure 6b), the

656 database of transactions is constructed by chunking this time series considering a fixed-length sliding

657 time window (Figure 6 (c)). Figure 6 (d) shows how the encoded transitions for each timestep are

658 stored in the database of transactions. For example, assuming a sliding window that includes four

659 timesteps, the database T can be represented by a $4 \: x \: n$ transition matrix where n corresponds to the

660 maximum number of sliding windows which can be contained in the time series of transitions.

661   Considering that the time windows are sliding a timestep by time, two consecutive rows in the

662   database T (Figure 6 (d)) differ only for a single item. As a reference considering a time series of

663   transitions with 6 timesteps and a sliding window that includes 4 timesteps, the database of

664   transactions is a 4×3 transition matrix given that the maximum number of complete time windows

665   is equal to 3 (Figure 6 (d)). After the construction of the database T, the temporal association rules

666   are searched among transactions.

667   The cSpade algorithm [51] has been selected for the extraction of the rules from the inter-transactional

668   database, setting in advance three fundamental parameters: minimum confidence, minimum support,

669   and maximum time lag between antecedent and consequent item sets (equal to the sliding window

670   length).

671   According to the proposed methodology, the first two parameters (i.e., confidence and support)

672   should be as high as possible, to ensure that the extracted rules are much frequent as possible and

673   then representative of the normal behaviour of the system.

674   Once the reference rule set has been identified, it is used for detecting the presence of potential faults

675   in a testing dataset.

676   In particular, a temporal association rule is expressed as a logical IF-THEN implication where the

677   presence of an event (i.e., antecedent) implies the occurrence of another event (i.e., consequent)

678   within a certain time lag. According to this formulation, three potential violations can occur when

679   such rules are applied on a testing set of data:

680   i)   absence of the antecedent itemset,

681   ii)   absence of consequent itemset,

682   iii)   absence of antecedent and consequent item sets.

683   In that perspective, the violation analysis helps physical interpretation of rules making it possible to

684   assess their sensitivity to the presence of specific faults or group of them.

685   In section 6.2, the results of the transient methodology herein described are presented and discussed

686   providing further details about the setting of the input parameters and the post-processing of the

687   extracted association rules.

688   ## 5.4   FDD methodology for the non-transient period

689   The methodology employed for performing the FDD analysis during non-transient period relies on

690   three fundamental phases that can be generalized as follows:

691   •   Development of reference models through classification trees, representative of the normal

692   behaviour (fault-free condition) of the system under analysis;

693   •   Comparison between the estimated behaviour of the system and the actual one (i.e., evaluation

694   of model residuals) for detecting potential faulty conditions;

695   •   Analysis of the model residuals for diagnosing the most probable cause associated to a specific

696   fault (fault diagnosis).

697   The first step of the process consists of a robust characterization of the fault free operation of the

698   AHU during the non-transient period (i.e., from 07:00 to 18:00). To this purpose, several estimation

699   models (i.e., classification trees) have been developed on a portion of the available non-transient

700   dataset. In detail 20 days tagged as fault-free were considered at this stage (training dataset) while the

701   remaining 2 fault-free days and 11 faulty days (testing dataset) were used in the successive diagnostic

702   phase.

703   For the development of the estimation models (i.e., classification trees), all the variables related to

704   the operation of the AHU (e.g., *supply fan power* (SF_WAT)*, return fan power* (RF_WAT)*, supply*

705   *air flow rate* (SA_CFM)) have been selected once at a time as target attribute while the remaining

706   ones have been used as input attributes. However, features related to external forcing variables to the

707   AHU system (i.e., *cooling coil input water temperature* (CHWC_EWT), *outdoor air temperature*

708   (OA_TEMP)) have been used only as input attributes.

709   In that way, 21 classification trees are developed for providing a robust benchmark of the fault-free

710   operation. To that purpose, a CART algorithm is employed as a supervised classifier in the study.

711   The developed classification trees estimate for each target variable and for each 15-min aggregation

712   interval included in the non-transient period the most probable discrete value (encoded as symbol)

713   according to the relationship that exists between all the input variables and the dependent attribute.

714   Successively all the classification trees developed are put together in the same estimation layer as

715   shown in Figure 7. At this stage, the estimation process can be summarized as follows:

716   • At each aggregation interval (i.e., 15 min.) the monitored variables are encoded into symbols

717   through the aSAX method (i.e., pre-processing stage);

718   • The set of encoded variables goes through the estimation layer (that consists of 21

719   classification trees) providing an estimation of each target variable for the considered

720   aggregation interval;

721   • The actual symbols are compared with the estimated ones.

722   The latter step consists in the evaluation of the model residuals.

723   In this study, the difference between two equal symbols is assumed to be zero, while the residual

724   differs from zero if the symbols are at least one alphabet apart. For example, if the estimated and

725   actual symbol for a variable is equal to "A" and "B" respectively, the residual between those symbolic

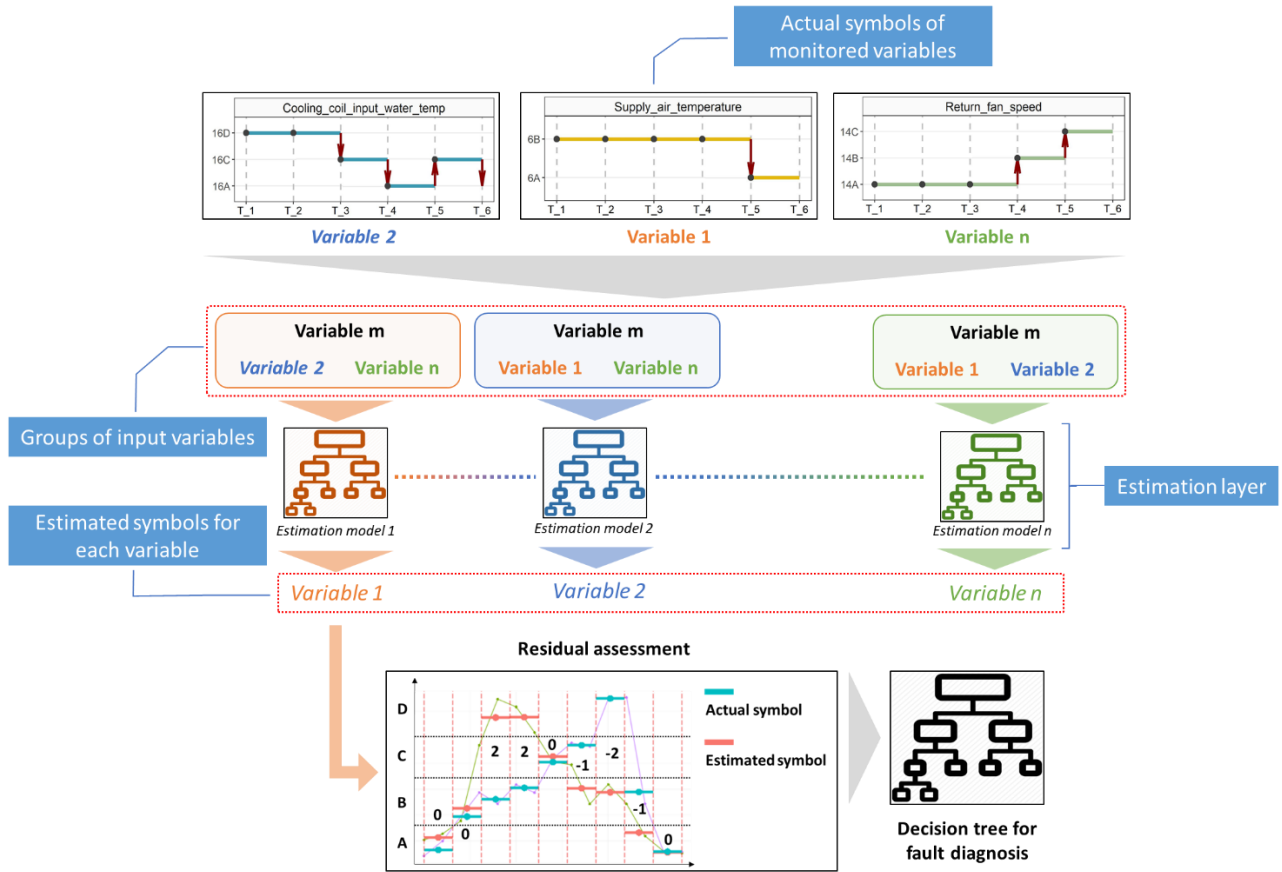726   discrete-values is equal to 1 (Figure 7).

727

Figure 7. Analytics module for the non-transient period.

Considering that the estimation models are trained on fault-free data, at the end of the estimation process it is possible to assess how much the input data differ from the reference fault-free behaviour of the AHU through the analysis of residuals. Understanding which variables are out of range and assessing the severity of those deviations enables the detection of possible faulty conditions. In order to test this FDD procedure, all the days excluded from the training set of the reference models (i.e., 2 fault-free days and 11 faulty days) have been considered. In particular, each day included in the testing dataset is labelled as "Normal" or with the tag of one of the faults reported in Table 1.

The time series of the 13 days are pre-processed (aggregated in intervals of 15-min and encoded in symbols) and put through the estimation layer (i.e., 21 classification trees) generating a dataset of residuals as shown in Figure 8. At this stage, a further classification tree has been developed to predict the label of each faulty or normal condition (Figure 8) for performing the fault diagnosis. This classification tree estimates the most probable label (e.g., CCVSFC, EASFC, RFCF or Normal) according to the residuals evaluated for each variable as an outcome of the estimation layer.

Aggregation interval	Day	Variable 1 Residual	Variable n Residual	Variable 21 Residual	Fault label
15:00 – 15:15	1	0	...	0	Normal
15:15 – 15:30	1	0	...	0	Normal
15:30 – 15:45	1	0	...	0	Normal
...	...	...	...	...	...
15:00 – 15:15	5	1	...	3	CCVSFC
15:15 – 15:30	5	0	...	-1	CCVSFC
15:30 – 15:45	5	-2	...	0	CCVSFC
...	...	...	...	...	...
15:00 – 15:15	10	2	...	1	EASFC
15:15 – 15:30	10	1	...	0	EASFC
15:30 – 15:45	10	0	...	-2	EASFC
...	...	...	...	...	...
15:00 – 15:15	13	-3	...	1	RFCF
15:15 – 15:30	13	1	...	-2	RFCF

Set of input variables of the classification tree   Target variable of the classification tree

Figure 8. Structure of the database used for developing the classification tree of fault diagnosis

In the dataset reported in *Figure 8* the target variable is the fault tag, and the same tag is assigned to all of the 44 aggregation intervals of 15-min that belong to the same day (included in the 11 hours of "non transient" operation of the AHU from 7:00 to 18:00), generating a total amount of 572 instances on which develop the classifier. The present methodology exploits the CART algorithm for developing the decision trees since it proved to be a good choice for fault diagnosis [19][66].

As already mentioned above, in this paper the developed FDD tool is trained and tested on real data of an AHU operated in non-transient cooling mode for 33 non-consecutive days during the summer season (22 "normal" days and 11 "faulty" days). Note that the decision and association rules extracted through the proposed supervised and unsupervised approaches can be considered valid only for the operation mode under consideration. In this perspective, rule-based tools can be easily integrated in FDD process with hierarchical architecture capable to exploit only the useful knowledge during specific conditions. For instance, the use of automatic detector makes it possible to call specific sets of rules depending on the operating mode of the AHU: off mode, heating mode, free cooling mode, and mechanical cooling mode [67].

In Section 6.3, the results of the non-transient methodology herein described are presented and discussed providing further details about the performance, reliability and generalizability of the entire process.

6 Results

6.1 Pre-processing stage

According to the methodological framework introduced in Section 5, a data preparation stage was preliminarily implemented. Firstly, outliers were filtered out by implementing the Hampel filter on the 1-minute time series. For each data sample of the time series, the filter computes the standard deviation and the median of a window composed of the current sample and $\frac{Len-1}{2}$ adjacent samples on each side of the current sample. *Len* is the window length and in this study is set equal to 31 minutes. A window with a length of 31 minutes could be not too much sensitive to the presence of outliers considering that the sample on which the standard deviation is computed is quite large. However, such window length proved to be suitable for identifying extremal values that certainly are related to problems of the sensing system. In the performed analysis, the filter does not take into account the first and the last *(Len-1)/2* data points of each daily time series. Such data points are always related to measurements during the hours when the AHU system is turned off (time intervals from 00:00 to 00:14 and from 23:45 to 23:59) and do not affect the results in any ways.

After data pre-processing (i.e., cleaning and replacement of outliers) a data reduction was performed by means of a PAA process with the aim of approximating the time series of each considered variable to the mean value calculated in non-overlapped time intervals with a fixed length of 15 min. The time interval length of 15 minutes was chosen as the best trade-off between approximation accuracy and data size reduction. Successively, the encoding of the reduced variables in symbols was carried out by implementing the aSAX algorithm [45].

The algorithm was initialised for each variable by identifying the number of symbols (i.e., discretization intervals) and the initial positions of the breakpoints (i.e., borders of the discretization intervals) with a hierarchical cluster analysis using the Ward linkage method [47]. Through the clustering algorithm, it was possible to obtain the optimal number of discretization intervals (i.e.,

785   number of symbols) by computing several cluster validation metrics. This process was completely

786   automated and performed through Nbclust package [68] available in the statistical software R. The

787   number of discretization intervals was constrained from 2 to 4 considering only data referred to the

788   period of operation of the system (i.e., ON-hours of the system).

789   When the optimal positions of the adaptive breakpoints were found and each variable was encoded

790   in symbols, the operation conditions of the AHU were considered fully characterised. Then, the data

791   related to OFF-hours of the system operation were analysed to find possible additional intervals. In

792   particular, if during OFF-hours a variable typically assumes values that are out of the identified ranges

793   of discretization, a new lower or upper half-open interval was appended to the previous ones.

794
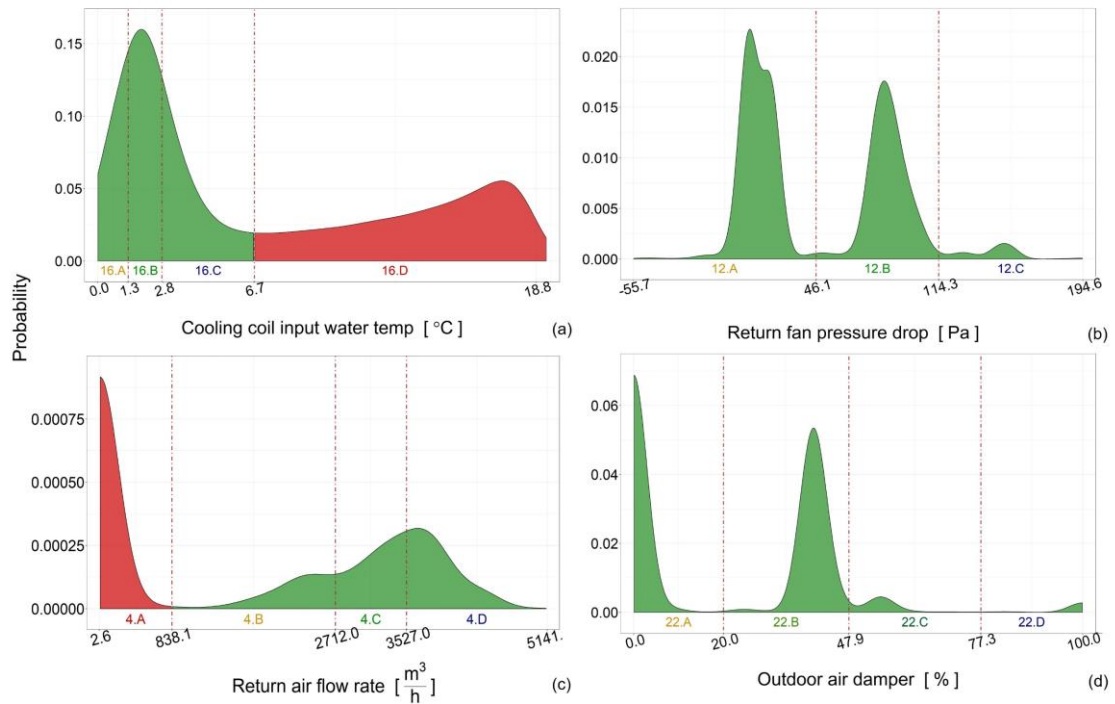
795 *Figure 9. Distributions and breakpoint identification for some variables.*

796 Figure 9 shows the encoding process performed for 4 variables (i.e., *cooling coil input water*

797 *temperature* (CHWC_EWT), *return fan pressure drop* (RF_DP), *return air flow rate* (RA_CFM),

798 *outdoor air damper position* (OA_DMPR)) randomly selected from the set of inputs. It can be

799 observed that for two variables an additional OFF-hours discretization interval (i.e., red area of the

800 distributions in Figure 9 (a) and (c)) was added to the other ranges of values for the symbol encoding

801 (i.e., ID n° = 16, symbol = D and ID n° = 4, symbol = A).

802 As a reference, Table A in Appendix A summarizes the transformation results obtained, with the

803 specification of the numerical range corresponding to each symbol for all the analysed operational

804 variables.

805 At this stage, according to the procedure described in Section 5.2, transient and non-transient periods

806 were identified and the data set was consequently segmented. In particular, the time interval between

807 5:00 and 7:00 was labelled as transient start-up period, while the period from 7:00 to 18:00 was

808 considered as non-transient period. The results obtained from the application of the methodological

809 framework are in the following presented and discussed separately for transient and non-transient

810 periods.

811 ## 6.2 Fault detection analysis for the transient period (system start-up)

812 According to the methodological process introduced in section 5, the encoded time series were

813 analysed for extracting temporal association rules in the start-up period of system operation. In detail,

814 the transitions of the variables (i.e., change from a symbolic discrete-value to another one) were

815 preliminarily encoded and the inter-transactional database was created considering a sliding window

816 of 60 minutes. The width of the sliding window was chosen to be large enough to include any effect

817 of the system dynamics, but tight enough to ensure that the occurrence of a consequent itemset was

818 related to a physics-based implication with its antecedent itemset.

819 Considering that the fault detection methodology was conceived for extracting reference association

820 rules of normal operation, the inter-transactional database was created from the fault-free dataset, by

821 selecting rules with high values of support and confidence.

822 Typically, the main issue related to association rules mining consists in handling and filtering the

823 large number of rules extracted and eventually identify those that are of interest [20]. To tackle this

824 problem and facilitate the mining of useful knowledge from extracted rules, a post-mining phase was

825 performed.

826   The post-mining phase was aimed at solving various practical issues, such as interestingness,

827   redundancy, generalization, visualization and interpretability of association rules.

828   To this purpose, additional quality metrics were introduced: the daily support of the rule (i.e.

829   SUPP.DAY) calculated for both fault-free (SUPP.DAY$_{NORMAL}$) and the faulty days

830   (SUPP.DAY$_{FAULTY}$) and the actual time lag between the antecedent and consequent of a rule

831   (ACTUAL TIME LAG). In more detail, the SUPP.DAY$_{NORMAL}$ is defined as the percentage of fault-

832   free days during which a single association rule (R_i) occurred, while SUPP.DAY$_{FAULTY}$ is calculated

833   for the faulty days (Eq. (5) and Eq. (6), respectively).

834

835
$$SUPP.DAY_{NORMAL}, R_i = \frac{\text{N° of Free−fault days with of the occurrence of the rule } R_i}{\text{Tot. N° of Free−fault days}} \tag{5}$$

836

837
$$SUPP.DAY_{FAULTY}, R_i = \frac{\text{N° of Faulty days with of the occurrence of the rule } R_i}{\text{Tot. N° of Faulty days}} \tag{6}$$

838   However, according to ASHRAE project RP-1312, during the faulty day tagged as CCVSFO (i.e.,

839   cooling coil valve stuck open), the blockage of the cooling valve in fully open position was

840   implemented from 8:00 to 18:00 and hence out of the start-up period of the system. For this reason,

841   the day tagged as CCVSFO has been not considered in the calculation of SUPP.DAY$_{FAULTY}$.

842   The ACTUAL TIME LAG was introduced to evaluate the most frequent temporal distance between

843   the first occurrence of an antecedent and the last occurrence of the corresponding consequent of a

844   specific rule. Consequently, even though the rules are searched with a sliding window of 60 minutes,

845   the user can have a feedback about the most frequent time interval within a consequent occurs given

846   the presence of its antecedent.

847   The ACTUAL TIME LAG was calculated for each rule by computing the cumulative frequency of

848   occurrences of the temporal distance between antecedent and consequent. For each rule a cumulated

849   frequency threshold of 80% was considered in order to evaluate this metric.

850 Figure 10 shows the frequency distribution of the ACTUAL TIME LAG for two rules. The rule on

851 the left (i.e., rule 1077) occurs for more than the 80% of the time with an actual time lag between the

852 antecedent itemset and consequent itemset of 15 minutes, while for the rule on the right (i.e., rule

853 15268) the 80% of occurrences has a characteristic time lag lower or equal to 30 minutes.

854
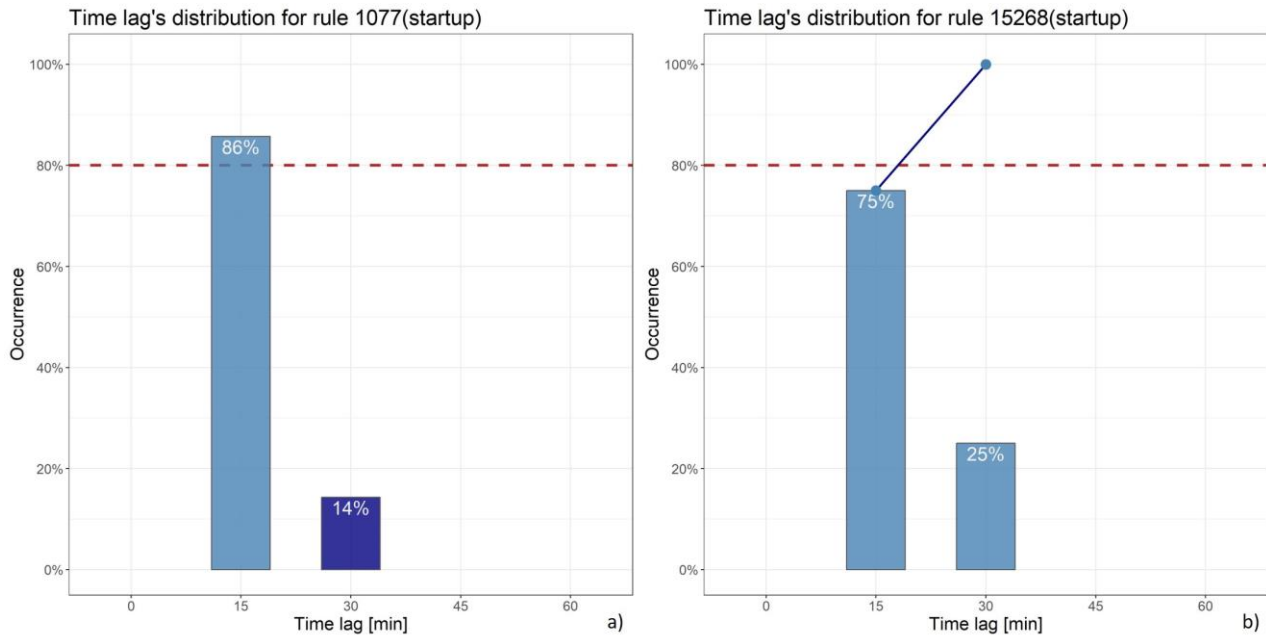
855

856 *Figure 10. Distribution of the time lags for rule 1077 (a) and rule 15268 (b) – (refer to Table B in Appendix A for the*

857 *description of the rules).*

858 At this stage, more than 15,000 rules were extracted from the start-up dataset of fault-free days (in

859 more or less 10 min.), assuming minimum support and minimum confidence equal to 0.7 and not

860 including drivers of system's operation as potential consequent events (i.e. *outdoor air temperature*

861 (OA_TEMP) and *cooling coil input water temperature* (CHWC_EWT)).

862 After the rule extraction, the values of support and confidence were recalculated considering only the

863 occurrences of each rule within the evaluated ACTUAL TIME LAG (instead of the window of 60-

864 min), reducing the set of rules to 7,419 rules.

865 Since the rules extracted should be representative of the fault-free operation of the system, only the

866 rules, which in the testing dataset frequently occur in normal days and rarely in the faulty ones, are

867 of interest for the problem under investigation. To this purpose, after the application of the 7,419

868   temporal association rules to the testing dataset, only the rules with a SUPP.DAY$_{NORMAL}$ equal to 1

869   (i.e., the rule occurring for each day labelled as "normal" included in the testing dataset) and a

870   maximum value of SUPP.DAY$_{FAULTY}$ equal to 0.3 were considered with the final result of obtaining

871   465 reference rules (SUPP.DAY values are set by the user).

872   As a general approach, the parameters were set in order to obtain a limited number of interesting

873   rules, which respect the following conditions i) each rule occurs during fault-free condition with high

874   support and confidence, ii) each rule has high probability to be violated during faulty conditions

875   regardless from the fault type.

876   In this perspective, general rules that are sensitive to more fault types at the same time were preferred

877   to those violated only for specific faults.

878   The introduced metrics allow an enhanced comprehension of the rule set, making it possible to

879   discriminate rules with high support and confidence occurring during both fault-free and faulty days,

880   from the rules, robust as well, occurring only during the normal operation of the system.

881   Figure 11 shows for each day in the testing dataset (composed by 11 different faulty days and 2

882   Normal days) the percentage of rules (out of the 465 considered) which occurred and/or have been

883   violated, with specification of the kind of violation detected. In particular, the label "*presence*"

884   indicates that the rule occurred with its antecedent and consequent while the labels "*antecedent*",

885   "*consequent*" and "*absence*" indicate three different types of violation. In detail, the label

886   "*antecedent*" denotes that a rule was violated because of the only presence of the antecedent; the label

887   "*consequent*" indicates that a rule was violated because of the only presence of the consequent; the

888   label "*absence*" indicates the complete violation of a rule because of the absence of both antecedent

889   and consequent. The characterisation of the rules in terms of type of violation helps the interpretation

890   of the path which determines a specific fault. In fact, the presence of the only antecedent, the only

891   consequent, rather than the absence of both item sets, correspond to different behaviours of the system

892   in relation to the presence of the considered faults.

893   The results obtained can be described according to the severity of rule violation for each day

894   representative of a specific fault implementation or normal operation. To this purpose four different

895   groups of days were identified and in the following described.
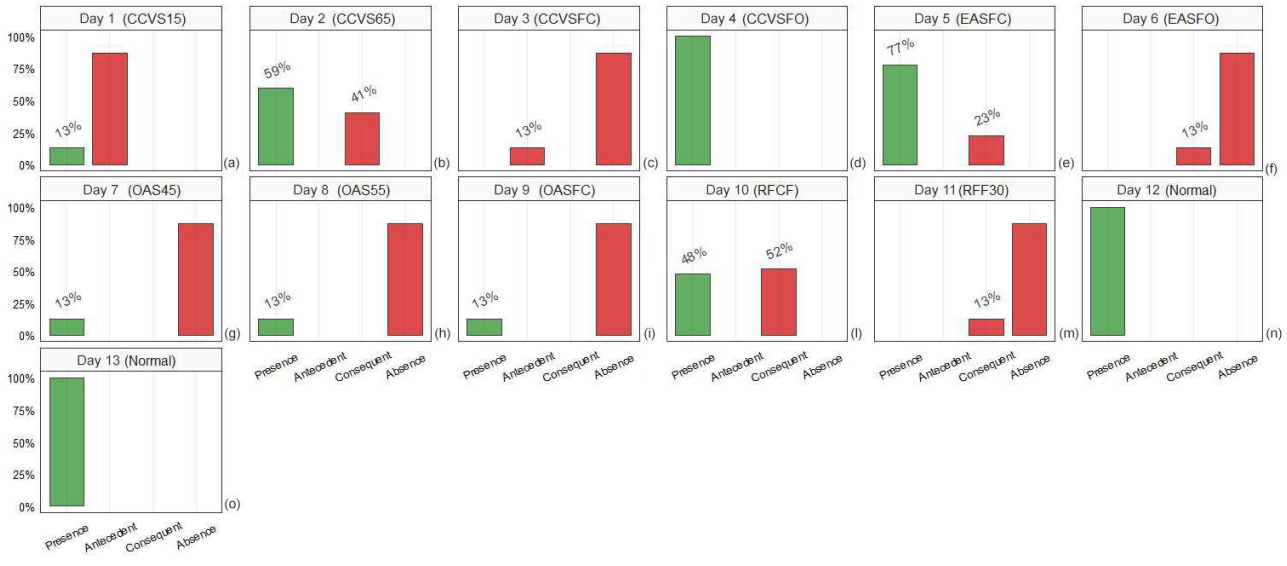
896

897   *Figure 11. Characterization of the presence or the violation of the extracted rules for the testing days (refer to Table 1*

898   *for the encoding of faults).*

899   The first group includes days characterized by the presence of the 100% of the 465 rules tested. This

900   is the case of days in Figure 11 (d), (n) and (o) tagged as Normal and the faulty day tagged as

901   CCVSFO. Such condition suggests, as expected, that during the faulty day CCVSFO the start-up of

902   the system can be considered normal.

903   The second group instead, includes the days in Figure 11 (a), (c), (f), (g), (h), (i) and (m) that are

904   characterized by a net prevalence of rule violations (more than 70%). Moreover, for those days, the

905   presence of a fault is also associated to a specific kind of violation of the rules. As a reference, in case

906   of CCVSFC, EASFO, OAS45, OAS55, OASFC and RFF30 the rules are violated mainly due to the

907   absence of both antecedents and consequents, while only in the in case of CCVS15 the rule was

908   violated for the absence of consequent.

909   The third group includes the day in Figure 11 (e) for which, during the start-up period, the percentage

910   of violations is lower than the percentage of valid occurrences of the rules. Such condition suggests

911   that during this day the behaviour of the system is similar to the normal one limiting the number of

912   violations occurred. The main reason is that such fault does not strongly affect the system operation

913   making the detection process less sensible to its presence. This result agreed with the findings of the

914   ASHRAE-RP 1312 project, during which the analysed dataset was generated [14].

915   The last group includes days in Figure 11 (b) and (l) that are characterized by a similar amount of

916   violated and not violated rules (violation rate between 40% and 60%). These two faults seem to affect

917   the performance of the system differently from other faults respect to which hypothetically should

918   exhibit high similarity (i.e., CCVS15 and RFF30). Regarding the fault CCVS65 (Figure 11 (b)), the

919   cooling coil valve is stuck open at 65% and therefore the supply air flow is overcooled. In this case,

920   the system reacts by opening the heating coil valve and operating in fully recirculation mode for

921   increasing the *supply air temperature* (SA_TEMP). Consequently, the failure of the cooling coil valve

922   does not affect the capability of the system in reaching the supply set-point temperature, but the

923   operation of the other components is different from the normal condition.

924   On the opposite, during the day (Figure 11 (a)) tagged as CCVS15 (included in group 2) the cooling

925   coil valve is almost closed limiting the heat transfer with the supply air flow that does not reach the

926   set point temperature. Such case is representative of the complete failure of the system in maintaining

927   the desired conditions of the indoor environment, as a matter of fact, justifying a higher rule violation

928   rate for CCVS15 respect to CCVS65.

929   Regarding the fault RFCF (Figure 11 (l)), the system is operated implementing the complete failure

930   of the return fan despite its speed control signal is correctly elaborated. Instead, during the day in

931   Figure 11 (m) tagged as RFF30 (included in group 2), the return fan is not corrupted, but it is subjected

932   to a faulty control signal. In this case the high number of rules violated for RFF30 suggests a higher

933   sensitivity of the extracted rules to frequent transitions of the fan speed discrete values rather than fan

934   power ones.

935   Some key figures related to the 465 extracted rules are described below. The rules are characterized

936   by an ACTUAL TIME LAG that lies between 15 and 30 minutes. The evaluation of the ACTUAL

937   TIME LAG can be considered as an essential step for reducing the intrinsic latency of the FDD

938   process during real implementation. Indeed, the ACTUAL TIME LAG gives the opportunity to check

939   the occurrence of a rule within a time interval smaller than the width of the sliding window used for

940   the rule extraction (in this case study, equal to 60 min.).

941   The transitions in the antecedent and consequent item sets are reported in Table 3 with the

942   corresponding occurrence frequency. In particular, the number of different consequent item sets is

943   13, resulting from a combination of 4 different events, while the antecedent item sets are 99, resulting

944   from the combination of 12 different events.

945   *Table 3. Occurrence frequency of each event included in the antecedent and consequent item sets*

Itemset	Variable	Event	Frequency
Antecedent	Return Fan Speed	RF_SPD [A-B]	87%
	Cooling coil input water temperature	CHWC_EWT [D-C]	31%
	Return fan power	RF_WAT [A-B]	24%
	Exhaust air damper position	EA_DMPR [A-B]	23%
	Cooling coil output water temperature	CHWC_LWT [C-B]	22%
	Supply fan speed	SF_SPD [A-B]	22%
	Cooling coil input water temperature	CHWC_EWT [C-A]	21%
	Supply fan power	SF_WAT [A-B]	21%
	Return fan start/stop signal	RF_SST [A-B]	18%
	Return air flow rate	RA_CFM [A-B]	16%
	Return fan pressure drop	RF_DP [A-B]	12%
	Return fan pressure drop	SF_DP [A-B]	9%
Consequent	Return Fan Speed	RF_SPD [B-C]	87%
	Supply Air Temperature	SA_TEMP [B-A]	49%
	Cooling coil output water temperature	CHWC_LWT [B-A]	46%
	Cooling coil air temperature	CHWC_DAT [B-A]	36%

946

947   The obtained rule set, including the most representative rules, is reported in Table B in Appendix A.

948   The rules extracted are meaningful since they can be interpreted as chains of events that characterise

949   the normal operation of the AHU in reaching the set-point conditions during the start-up period.

950   Indeed, extracted rules can be expressed as IF-THEN implications to be verified within a specific

951   time interval. As a reference, the rule n° 8661 (included in Table B in Appendix A) can be written

952   and interpreted as follow: IF (RF_SPD [A-B] and CHWC_LWT [C-B] and EA_DMPR [A-B]) occur

953   THEN (CHWC_DAT [B-A] and RF_SPD [B-C]) will occur within 30 minutes with the 100% of

954   confidence during a normal day.

955   In detail, the antecedent itemset includes transitions related to the return fan speed (RF_SPD), the

956   *cooling coil output water temperature* (CHWC_LWT) and the *exhaust air damper position*

957   (EA_DMPR) that imply the occurrence of consequent transitions related to *cooling coil output water*

958   *temperature* (CHWC_LWT) and *return fan speed* (RF_SPD).

959   In order to further improve the interpretability of the rules a novel visualization was proposed in this

960   work. An example of this visualization is showed in Figure 12, where the profiles of the variables

961   involved in rule n°1253 (see Table B in Appendix A).

962   Figure 12 shows the trend of the variables in terms of real profile (i.e. green curve) and PAA (i.e.

963   black segments). Regardless of the approximation introduced by the PAA, the behaviour of the

964   variables during the transient period is preserved, as can be seen by looking at the *supply air*

965   *temperature* trend (SA_TEMP). In fact, during the start-up period the *supply fan speed* (SF_SPD)

966   initially ramps up and then it is reduced to a constant level. The transitions of the antecedent itemset

967   are reported in red, while the consequent itemset in blue. The PAA is represented in a window of 60

968   minutes, while with a darker shade of grey the length of the ACTUAL TIME LAG (i.e., 15 minutes)

969   is reported. On the y-axis are shown the values used for the discretization of each variable.

970   The rule in Figure 12 shows a typical behaviour of the system at the start-up period, in terms of the

971   variation of *supply fan speed* (SF_SPD), *exhaust air damper* (EA_DMPR), *return fan power*

972   (RF_WAT), and *supply air temperature* (SA_TEMP).
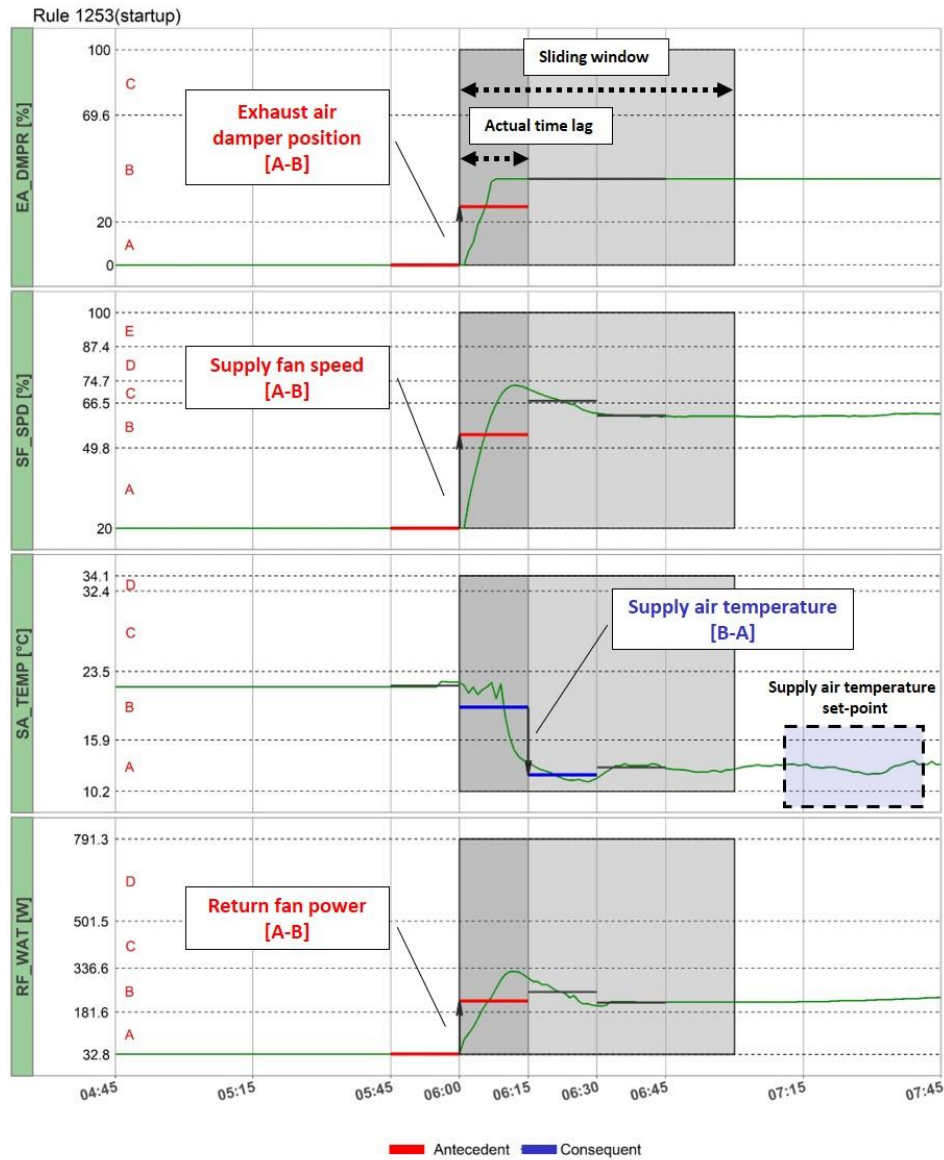
Figure 12. Visualization of an extracted temporal association rule (refer to Table 2 for variable encoding).

According to this rule, usually at the time scheduled for the start-up (i.e. 6:00 a.m.), the supply fan receives the start signal contemporary to the opening of the exhaust air damper while the *return fan power* (RF_WAT) increases (change from A to B). After 15 minutes from the occurrence of the first antecedent transition in the event chain, according to the rule, the *supply air temperature* (SA_TEMP) decreases from symbolic discrete-value B to A until the reaching of the desired set-point.

This proved that the chain of events related to each association rule provides information about the expected behaviour in terms of discrete-value changes among influencing variables of the AHU during normal operation.

6.3 Fault detection and diagnosis during non-transient period

984 In this section, the results obtained for the application of the methodology during non-transient period

985 described in section 5 are presented. The first step is aimed at developing a CT reference model for

986 each variable to predict the normal operation of the system. For the development of these reference

987 estimation models, all the variables related to the operation of the AHU have been selected once at a

988 time as target attribute while the remaining ones have been used as input attributes. However, features

989 related to external forcing variables to the AHU system (i.e., *cooling coil input water temperature*

990 (CHWC_EWT), *outdoor air temperature* (OA_TEMP)) have been used only as input attributes. As a

991 result, 21 reference models were built for providing a robust benchmark of fault-free operation.

992 Moreover, the variables used as input were also considered with a maximum backward lag of four

993 time steps (i.e. 60 minutes). Indeed, the decision trees are able to predict the discrete values (i.e.,

994 symbol) of a target variable considering the discrete values of the input variables both in the same

995 and previous aggregation intervals.

996
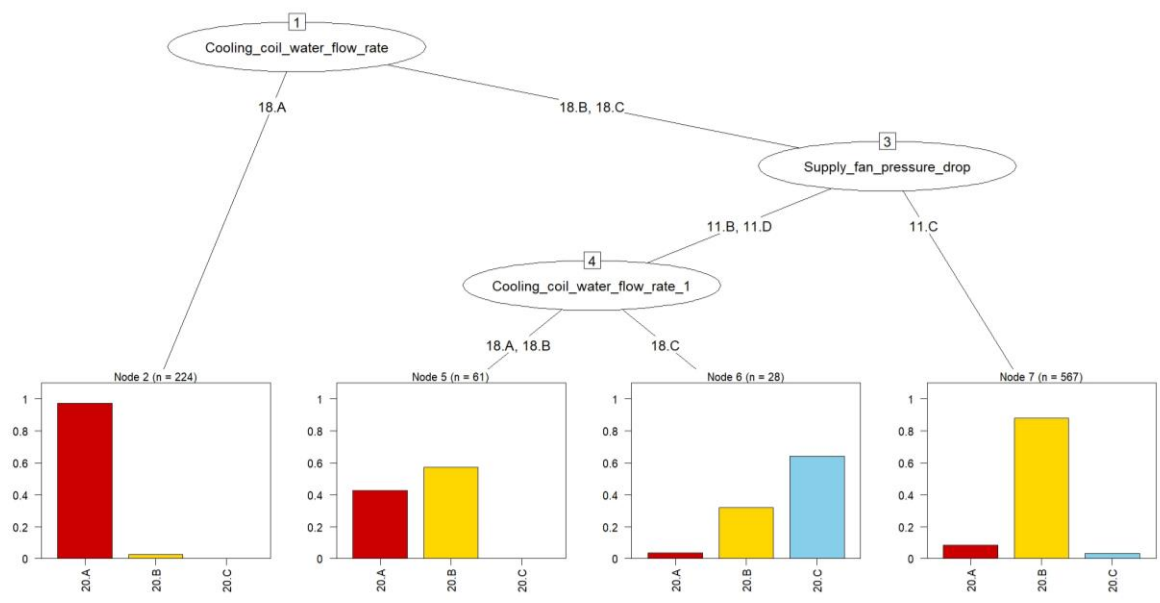
997 *Figure 13. Classification tree for the estimation of the symbolic discrete-values of the cooling coil valve position*

998 *(CHWC_VLV).*

999 Figure 13 reports as an example the CT model developed for predicting the discrete values (i.e.,

1000 symbol) of the variable *cooling coil water valve position* (i.e., variable tagged as CHWC_VLV with

1001   ID n° = 20), with an overall accuracy of 88% evaluated as the fraction of correct predictions with

1002   respect to the total number of predictions. The algorithm selected as input variables the *cooling coil*

1003   *water flow rate* (i.e., variable tagged as CHWC_GPM with ID n° = 18) and the *pressure drop of the*

1004   *supply fan* (i.e., variable tagged as SF_DP with ID n° = 11). From this CT, it is possible to extract

1005   useful decision rules for straightforwardly characterizing all the implications between discrete values

1006   (i.e., symbols) that typically occur during the fault-free operation of the AHU. Table 4 reports all the

1007   IF-THEN decision rules extracted from the CT shown in Figure 13 with the evidence of the accuracy

1008   achieved in each leaf node. The accuracy refers to each single leaf node assuming that the predicted

1009   label of the node corresponds to the label of the majority of the objects.

1010   For example, according to rule 4, the value of the response variable *cooling coil valve position* is

1011   equal to 20_B (i.e. CHWC_VLV lies in the interval 41 – 75 [%]) if the *cooling coil water flow rate*

1012   is equal to 18_B or 18_C (i.e. CHWC_GPM lies in the interval 0,89 – 2.7 [m^3/h]) and the *supply fan*

1013   *pressure drop* is equal to 11_C (i.e. SF_DP lies in the interval 562 – 770 [Pa]).

1014   *Table 4. Decision rules for the estimation of the symbolic discrete-value of cooling coil valve position (CHWC_VLV).*

Rule number	Decision rules	CHWC_VLV discrete-value	N° of objects	Leaf node accuracy
1)	**IF** CHWC_GPM = 18_A	20_A	224	95%
2)	**IF** CHWC_GPM = 18_B or 18_C **AND** SF_DP = 11_B or 11_D **AND** CHWC_GPM (lag -1) = 18_A or 18_B	20_B	61	55%
3)	**IF** CHWC_GPM = 18_B or 18_C **AND** SF_DP = 11_B or 11_D **AND** CHWC_GPM (lag -1) = 18_C	20_C	28	65%
4)	**IF** CHWC_GPM = 18_B or 18_C **AND** SF_DP = 11_C	20_B	567	85%

1015   Once all the estimation models were trained and validated, the residual analysis was performed by

1016   using a testing dataset including both faulty and fault-free data (i.e., 2 fault-free and 11 faulty days).

1017   Therefore, the difference between the actual status of a variable and that estimated by the CT during

1018   a aggregation interval determines the detection or not of a potential faulty condition, since the

1019   predicted status should be considered as the reference condition (fault-free). The values of the

1020   residuals can be equal to zero in case of absence of deviation from the normal conditions, positive if

1021   the actual value is higher than expected, while negative if the actual value is lower than expected.

1022   Eventually, in order to perform fault diagnosis, an additional CT model was developed, which uses

1023   in input the residuals obtained from the estimation performed through the previously described

1024   reference models and as output the tags related to the various faults analysed in this study.

1025   Figure 14 shows the classification model obtained, which can classify the faults considered with a set

1026   of intuitive rules, reaching an overall accuracy of the 90%.

1027
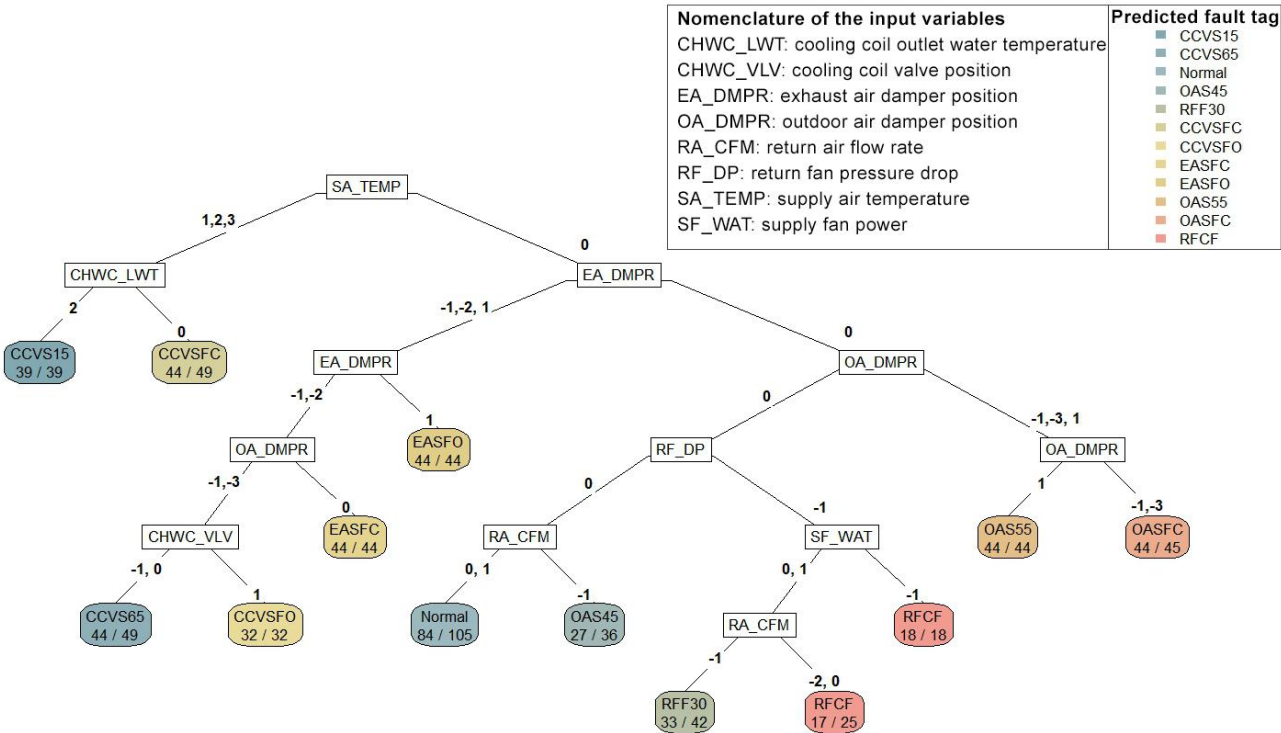
1028   *Figure 14. Classification tree for the fault diagnosis during the non-transient period.*

1029   The variables involved in input for the classification are the *supply air temperature* (SA_TEMP), the

1030   *outdoor air damper position* (OA_DMPR), the *exhaust air damper position* (EA_DMPR), the *cooling*

1031   *coil outlet water temperature* (CHWC_LWT), the *cooling coil valve position* (CHWC_VLV), the

1032   *supply fan power* (SF_WAT), the return *fan pressure drop* (RF_DP) and the *return air flow rate*

1033   (RA_CFM). The CT developed can diagnose 11 different faults and the normal condition as well.

1034   The latter is predicted by following the path of the CT (Figure 14) that includes all zeros (i.e. residual

1035   equal to zero) in the splits for the variables SA_TEMP, EA_DMPR, OA_DMPR, RF_DP and

1036   RA_CFM. With reference to Figure 14, some other rules are described in the following.

1037   The first split made by the CT algorithm is driven by the *supply air temperature* (SA_TEMP), which

1038   identifies the faults due to a blockage of the cooling coil valve at 0% (CCSFC) or at 15% (CCVS15)

1039   if the air temperature presents higher values than normal (i.e., SA_TEMP residuals = 1, 2, 3).

1040   In some cases, the faults can be diagnosed by analysing the variables directly related to the corrupted

1041   component, such as the blockage of the exhaust and outdoor air dampers at 0%, 55% or 100% (i.e.

1042   OASFC, OAS55, EASFC, and EASFO). In other cases, a series of deviation from the normal

1043   condition for different variables are considered as symptoms for a specific fault. That is the case, for

1044   example, of anomalous energy transfer in the cooling coil due to blockage of the cooling coil valve

1045   at 65% (CCVS65) or 100% (CCVSFO). These faults are diagnosed in the case both the air dampers

1046   are completely closed (i.e. negative values of residuals), but the *supply air temperature* (SA_TEMP)

1047   does not present a deviation from the normal condition. In this case, the system tries to counterbalance

1048   the excessive decrease of the temperature of the air by operating in fully recirculation mode.

1049   The effect of a fault related to the return fan (Figure 14) can be easily identified, since the pressure

1050   drop at the return fan is reduced, with the absence of deviation, from normal condition, for *supply air*

1051   *temperature* (SA_TEMP) and air dampers.

1052   The discrimination between the *return fan complete failure* (RFCF) and the case when the speed is

1053   fixed at 30% (RFF30) can be performed by evaluating the severity of the reduction of the *return air*

1054   *flow rate* (RA_CFM) rather than the reduction of the *supply fan power* (SF_WAT).

1055   The introduced FDD tool is a multiclass classifier and when in operation sorts data into either fault-

1056   free (i.e., normal) or faulty classes.

1057   All the evaluation metrics for a multiclass classification model can be understood in the context of a

1058   binary classification model (where the classes are "positive" and "negative"). These metrics are

1059   derived from the following categories:

1060   - True Positives (TP): Objects labelled as positive and predicted to be positive.

1061   - False Positives (FP): Objects labelled as negative and predicted to be positive.

1062   - True Negatives (TN): Objects labelled as negative and predicted to be negative.

1063   •   False Negatives (FN): Objects labelled as positive and predicted to be negative.

1064 The multiclass classification problem can be seen as a set of many binary classification problems and

1065 its performance can be assessed labelling as "positive" each class once at time. In the context of the

1066 presented multiclass FDD classifiers some metrics have been calculated:

1067   •   Accuracy (A): Objects of items correctly identified as either truly positive or truly negative

1068   out of the total number of items i.e., $(TP + TN)/(TP + TN + FP + FN)$.

1069   •   Recall (R): Number of objects correctly identified as positive out of the total actual positives

1070   i.e., $TP/(TP + FN)$. The recall is calculated for each class and then averaged among classes

1071   for a global performance assessment of the CT.

1072   •   Precision (P): Number of objects correctly identified as positive out of the total items

1073   predicted as positive i.e., $TP/(TP + FP)$. The precision is calculated for each class and then

1074   averaged among classes for a global performance assessment of the CT.

1075   •   False Positive Rate (FPR), Type I error: Number of objects wrongly identified as faulty out

1076   of the total actual fault-free data i.e., $FP/(FP + TN)$. In FDD processes, this error means that

1077   data belonging to fault-free class (negative) are incorrectly labelled as faulty (positives)

1078   generating false alarms.

1079   •   False Negative Rate (FNR), Type II error : Number of objects wrongly predicted as fault-free

1080   out of the total actual faulty data i.e., $FN/(FN + TP)$. In FDD processes, this error means that

1081   data belonging to one of the fault classes (positives) are incorrectly labelled as fault-free

1082   (negative) generating missing detection opportunities.

1083 The developed CT exhibits the following performances A = 90%, R = 89%, P = 91%, FNR = 4%,

1084 FPR = 4%. The performance of the CT can be also assessed with the detail of each class considered.

1085 To this purpose, in Table 5 is reported the Confusion Matrix (CM) of the CT. The CM, in form of

1086 table (actual class vs predicted class), allows an effective analysis of the performance of the CT

1087 algorithm making it possible to identify confusion between all the considered classes (i.e.,

1088 mislabelling of objects belonging to a class and classified into another one).

1089   In particular, rows of the table correspond to the actual classes while columns to the predicted ones.

1090   At this stage it is possible to evaluate in each class the proportion of prediction actually correct (i.e.,

1091   Precision) and the proportion of actual values predicted correctly (i.e., Recall).

1092   *Table 5. Precision and recall for classification tree of fault diagnosis during non-transient period.*

	CCVS15	CCVS65	Normal	OAS45	RFF30	CCVSFC	CCVSFO	EASFC	EASFO	OAS55	OASFC	RFCF	Total	Recall
CCVS15	**39**	0	0	0	0	5	0	0	0	0	0	0	44	89%
CCVS65	0	**44**	0	0	0	0	0	0	0	0	0	0	44	100%
Normal	0	0	**84**	3	0	0	0	0	0	0	1	0	88	96%
OAS45	0	0	17	**27**	0	0	0	0	0	0	0	0	44	61%
RFF30	0	0	2	1	**33**	0	0	0	0	0	0	8	44	75%
CCVSFC	0	0	0	0	0	**44**	0	0	0	0	0	0	44	100%
CCVSFO	0	5	2	5	0	0	**32**	0	0	0	0	0	44	73%
EASFC	0	0	0	0	0	0	0	**44**	0	0	0	0	44	100%
EASFO	0	0	0	0	0	0	0	0	**44**	0	0	0	44	100%
OAS55	0	0	0	0	0	0	0	0	0	**44**	0	0	44	100%
OASFC	0	0	0	0	0	0	0	0	0	0	**44**	0	44	100%
RFCF	0	0	0	0	9	0	0	0	0	0	0	**35**	44	80%
Total	39	49	105	36	42	49	32	44	44	44	45	43	572	**Average 89%**
Precision	100%	90%	80%	75%	79%	90%	100%	100%	100%	100%	98%	81%	**Average 91%**	

1093

1094   Thanks to the methodology introduced in the present paper the faults in the dataset were diagnosed

1095   with both high precision and recall, as can be seen in Table 5. The lowest values of precision and

1096   recall are related to the fault *outdoor air damper stuck at 45%* (OAS45), for which part of the records

1097   have been mislabelled as "Normal" (i.e., 17 out of 44 objects, that correspond to the 39% of data

1098   labelled as OAS45 and to the 89% of the total amount of False Negatives). This condition is due to

1099   the fact that the outdoor air damper stuck open at 45% does not invalidate the operation of the system

1100   which is similar to the fault-free one during the non-transient period. It is worth nothing that all the

1101   assumptions taken, and results obtained are related to a specific operative condition of the system

1102   (i.e., cooling mode). The set of rules extracted can be then considered a valid FDD solution if only

1103   applied on data consistent with the initial hypotheses. Despite this, even though the analysis is related

1104   to a portion of the possible operative conditions of an AHU, the performance achieved suggests good

1105   perspectives in applicability and generalizability of the proposed methodology.

7   Discussion and concluding remarks

The paper introduces a data-driven based methodology to perform an AFDD in AHUs. Two different analytics modules were proposed for transient and non-transient conditions of the AHU operation and consequently to enhance the energy performance of the ventilation and air-conditioning process. The dataset used for testing the methodology includes several faulty and fault-free running conditions related to the cooling operative mode of AHUs. Data were gathered from monitoring campaign on two identical AHUs in the framework of the Research Project ASHRAE RP-1312.

The fault detection during the start-up period was performed with an innovative approach by searching frequent and non-anomalous relationships between events in a temporal transaction set using temporal association rules. A temporal association rule is expressed as a logical IF-THEN implication where the presence of an event (i.e., antecedent) implies the occurrence of another event (i.e., consequent) within a certain time lag. According to this approach, in the analysed case study the violation of a rule or group of rules may suggest the occurrence of abnormal conditions during system operation. Three potential rule violations have been considered for detecting faults during the start-up period: i) absence of the antecedent, ii) absence of consequent, iii) absence of antecedent and consequent.

The used rules are extracted by expert knowledge from a large set of possible rules and are representative of the normal operation of the AHU and are characterised by high physical interpretability. The introduction of innovative parameters (e.g. SUPP.DAY in faulty and normal conditions, support and confidence in the ACTUAL TIME LAG) allowed a robust selection of the most interesting association rules, minimising the effort required in the post-processing stage. Furthermore, an effective visualization of the temporal association rules was introduced with the aim of supporting energy managers in the interpretation of the temporal associations between operational variables in real-time.

The AFDD during non-transient period was performed by training and testing 21 CT models for providing a robust benchmark of the fault-free operation. The CT models are able to predict the

1132   discrete values of a target operational variable considering the values of the input variables both in

1133   the same and previous aggregation interval. The CTs showed high performance (i.e., high accuracy,

1134   precision and recall) in modeling all the variable relations that are characteristic of the operative

1135   condition of interest (i.e., 20 days of AHU operated in cooling mode).

1136   Eventually, an additional CT was developed in order to perform fault diagnosis. The model showed

1137   an overall accuracy of 90% and consists of a set of intuitive rules easy to be implemented for detecting

1138   up to 11 typical faults in AHUs. However, the set of rules extracted can be then considered as a valid

1139   FDD solution only if applied on data consistent with the initial hypotheses (i.e., AHU operated in

1140   cooling mode).

1141   Overall, the results obtained are characterised by robustness and high interpretability proving the

1142   effectiveness of the proposed methodology for ensuring a correct energy and operational management

1143   of the ventilation and air-conditioning process.

1144   Even though the rule set and the classification models are tailored for the case study analysed, the

1145   outcomes of the process can be considered flexible and generalizable. The methodologies were

1146   conceived for being automatic and for effectively managing the redundancy, interpretability and

1147   physical meaningfulness of the association and classification rules. Moreover, the proposed AFDD

1148   process is conceived for quasi real-time implementation, also minimising the user contribution and

1149   paying attention to the optimisation of computational cost. To this purpose, the preliminary

1150   discretisation of the variables, performed trough the aSAX algorithm, proved to be particularly

1151   effective in extracting the crucial operational conditions of the AHU reaching the optimal trade-off

1152   between data reduction and information loss. Moreover, the association rules were extracted from an

1153   event-based dataset (i.e., database of transactions) where only information about the discrete-value

1154   changes of the operational variables is stored. As a consequence, the computational cost related to

1155   the mining of rules is strongly reduced, increasing the feasibility of such approach in real case studies.

1156   As a reference the whole analytics process takes about 45 min in terms of computational time on a

computer equipped with quad-core processor Intel i7-3632QM CPU (2.20GHz) and 8GB RAM DDR4. In more detail the rule extraction phase takes more or less 10 minutes. It means that the most onerous parts of the analysis are represented by the pre-processing and post-mining phases. In the pre-processing phase the assessment of the optimal quantization of the time series through aSAX is validated by using more than 20 metrics (cluster validity indices included in the R Nbclust package [68]). Such calculation takes more than 10 minutes. In the post mining phase, the recalculation of support and confidence of each rule within the evaluated ACTUAL TIME LAG (instead of the window of 60-min), and the violation analysis performed on the testing dataset take about 20 minutes. For what concern the analysis of non-transient data, the development of each classification tree takes few seconds of computation and can be considered a task easily parallelizable. As a result, the impact of the analysis of non-transient data can be considered negligible in terms of computational cost compared to the pre-processing, rule extraction and rule post-mining. Indeed, in the perspective of a real-time implementation of the whole AFDD process, the update of the discretization intervals, set of association rules and estimation models can be accomplished during night-time while the fault detection and diagnosis tool can be run online during operation. For what concern the pre-processing stage, during the real-time operation the Hampel filter can still be used but considering that its intrinsic latency equal to *(Len-1)/2* should be added to the latency of the FDD process in detecting faults (in this case study the latency of the FDD process is equal to the length of the aggregation interval i.e., 15 min). For avoiding high latency in the analysis, *Len* can be reduced. As an alternative, other pre-processing algorithms, particularly suitable for the analysis of data streams, can be employed for detecting statistical outliers in real-time (i.e., before time $t + 1$ and without any look ahead) [71]. Further research will be then conducted to assess the scalability of the methodology to other operation modes and systems and to integrate it with knowledge driven-based analysis for better addressing the implementation issues characteristic of data-driven tools. Indeed, data-driven based FDD tools need a proper amount of data for the development of diagnosis models and cannot extrapolate beyond the range of training data [10]. It means that their capability in automatically

1183 extracting pattern from actual performance data is strictly related to the availability of pre-labelled

1184 monitored data (typically derived from AHU recommissioning or simulated data). On the contrary,

1185 knowledge driven-based approach can introduce domain knowledge and user experience into the

1186 FDD process [10], especially in the case initial information is not enough for deploying a data-driven

1187 process. In this perspective, a perfect integration of both approaches represents the main opportunity

1188 for significantly improve robustness, accuracy and generalizability of FDD tools conceived for

1189 application in building energy systems.

8   Acknowledgements

References

1196 [1]   A. Capozzoli, T. Cerquitelli, M.S. Piscitelli, Chapter 11 – Enhancing energy efficiency in

1197   buildings through innovative data analytics technologies, in: D. Ciprian, F. Xhafa (Eds.),

1198   Pervasive Comput., 2016: pp. 353–389. https://doi.org/10.1016/B978-0-12-803663-1.00011-

1199   5.

1200 [2]   L. Pérez-Lombard, J. Ortiz, C. Pout, A review on buildings energy consumption information,

1201   Energy Build. 40 (2008) 394–398. https://doi.org/10.1016/j.enbuild.2007.03.007.

1202 [3]   Office of Energy Efficiency & Renewable Energy (EERE) U.S. Department of Energy, DOE

1203   Office of Energy Efficiency and Renewable Energy, Buildings energy databook, 2012.

1204   http://buildingsdatabook.eren.doe.gov/DataBooks.aspx.

1205 [4]   J. Proctor, Residential and Small Commercial Central air Conditioning; Rated Efficiency isn't

1206   Automatic, Present. Public Sess. ASHRAE Winter Meet. (2004).

1207 [5]   K. Yan, C. Zhong, Z. Ji, J. Huang, Semi-supervised learning for early detection and diagnosis

1208 of various air handling unit faults, Energy Build. 181 (2018) 75–83.

1209 https://doi.org/10.1016/j.enbuild.2018.10.016.

1210 [6] R. Isermann, Fault-Diagnosis Systems: an introduction from fault detection to fault tolerance,

1211 Springer Science & Business Media, 2006. https://doi.org/10.1007/3-540-30368-5.

1212 [7] J. Granderson, G. Lin, R. Singla, E. Mayhorn, P. Ehrlich, D. Vrabie, Commercial Fault

1213 Detection and Diagnostics Tools: What They Offer, How They Differ, and What's Still

1214 Needed, 2018. https://doi.org/10.20357/B7V88H.

1215 [8] H. Kramer, G. Lin, J. Granderson, C. Curtin, E. Crowe, Synthesis of Year One Outcomes in

1216 the Smart Energy Analytics Campaign Building Technology and Urban Systems Division,

1217 (2017).

1218 [9] W. Kim, S. Katipamula, A review of fault detection and diagnostics methods for building

1219 systems, Sci. Technol. Built Environ. 24 (2018) 3–21.

1220 https://doi.org/10.1080/23744731.2017.1318008.

1221 [10] Y. Zhao, T. Li, X. Zhang, C. Zhang, Artificial intelligence-based fault detection and diagnosis

1222 methods for building energy systems: Advantages, challenges and the future, Renew. Sustain.

1223 Energy Rev. 109 (2019) 85–101. https://doi.org/10.1016/j.rser.2019.04.021.

1224 [11] C. Fan, F. Xiao, Z. Li, J. Wang, Unsupervised data analytics in mining big building operational

1225 data for energy efficiency enhancement: A review, Energy Build. 159 (2018) 296–308.

1226 https://doi.org/10.1016/j.enbuild.2017.11.008.

1227 [12] Y. Yu, D. Woradechjumroen, D. Yu, A review of fault detection and diagnosis methodologies

1228 on air-handling units, Energy Build. 82 (2014) 550–562.

1229 https://doi.org/10.1016/j.enbuild.2014.06.042.

1230 [13] A. Beghi, R. Brignoli, L. Cecchinato, G. Menegazzo, M. Rampazzo, F. Simmini, Data-driven

1231 Fault Detection and Diagnosis for HVAC water chillers, Control Eng. Pract. 53 (2016) 79–91.

1232 https://doi.org/10.1016/j.conengprac.2016.04.018.

1233 [14] S. Wen, Jin; Li, ASHRAE 1312-RP Tools for Evaluating Fault Detection and Diagnostic

Methods for Air-Handling Unit [FINAL REPORT], (2011) 13. http://marketingdatabase.tat.or.th/download/article/research/1201finalreport.pdf.

[15] D. Dehestani, F. Eftekhari, Y. Guo, S. Ling, S. Su, H. Nguyen, Online Support Vector Machine Applicationfor Model Based Fault Detection and Isolationof HVAC System, Int. J. Mach. Learn. Comput. 1 (2011) 66–72. https://doi.org/10.7763/ijmlc.2011.v1.10.

[16] Y. Zhao, J. Wen, F. Xiao, X. Yang, S. Wang, Diagnostic Bayesian networks for diagnosing air handling units faults – part I: Faults in dampers, fans, filters and sensors, Appl. Therm. Eng. 111 (2017) 1272–1286. https://doi.org/10.1016/j.applthermaleng.2015.09.121.

[17] Y. Zhao, J. Wen, S. Wang, Diagnostic Bayesian networks for diagnosing air handling units faults - Part II: Faults in coils and sensors, Appl. Therm. Eng. 90 (2015) 145–157. https://doi.org/10.1016/j.applthermaleng.2015.07.001.

[18] T. Mulumba, A. Afshari, K. Yan, W. Shen, L.K. Norford, Robust model-based fault diagnosis for air handling units, Energy Build. 86 (2015) 698–707. https://doi.org/10.1016/j.enbuild.2014.10.069.

[19] R. Yan, Z. Ma, Y. Zhao, G. Kokogiannakis, A decision tree based data-driven diagnostic strategy for air handling units, Energy Build. 133 (2016) 37–45. https://doi.org/10.1016/j.enbuild.2016.09.039.

[20] M.K. Mchugh, Data-Driven Leakage Detection in Air-Handling Units on a University Campus, ASHRAE Annu. Conf. (2019).

[21] Z. Yu, F. Haghighat, B.C.M. Fung, L. Zhou, A novel methodology for knowledge discovery through mining associations between building operational data, Energy Build. 47 (2012) 430–440. https://doi.org/10.1016/j.enbuild.2011.12.018.

[22] P. Xue, Z. Zhou, X. Fang, X. Chen, L. Liu, Y. Liu, J. Liu, Fault detection and operation optimization in district heating substations based on data mining techniques, Appl. Energy. 205 (2017) 926–940. https://doi.org/10.1016/j.apenergy.2017.08.035.

[23] C. Zhang, X. Xue, Y. Zhao, X. Zhang, T. Li, An improved association rule mining-based

method for revealing operational problems of building heating, ventilation and air conditioning (HVAC) systems, Appl. Energy. 253 (2019) 113492. https://doi.org/10.1016/j.apenergy.2019.113492.

[24] C. Fan, F. Xiao, H. Madsen, D. Wang, Temporal knowledge discovery in big BAS data for building energy management, Energy Build. 109 (2015) 75–89. https://doi.org/10.1016/j.enbuild.2015.09.060.

[25] C. Fan, Y. Sun, K. Shan, F. Xiao, J. Wang, Discovering gradual patterns in building operations for improving building energy efficiency, Appl. Energy. 224 (2018) 116–123. https://doi.org/10.1016/j.apenergy.2018.04.118.

[26] A. Capozzoli, F. Lauro, I. Khan, Fault detection analysis using data mining techniques for a cluster of smart office buildings, Expert Syst. Appl. 42 (2015) 4324–4338. https://doi.org/10.1016/j.eswa.2015.01.010.

[27] I. Khan, A. Capozzoli, S.P. Corgnati, T. Cerquitelli, Fault detection analysis of building energy consumption using data mining techniques, Energy Procedia. 42 (2013) 557–566. https://doi.org/10.1016/j.egypro.2013.11.057.

[28] M. Dey, S.P. Rana, S. Dudley, Smart building creation in large scale HVAC environments through automated fault detection and diagnosis, Futur. Gener. Comput. Syst. (2018). https://doi.org/10.1016/j.future.2018.02.019.

[29] Z. Du, X. Jin, Y. Yang, Fault diagnosis for temperature, flow rate and pressure sensors in VAV systems using wavelet neural network, Appl. Energy. 86 (2009) 1624–1631. https://doi.org/10.1016/j.apenergy.2009.01.015.

[30] Z. Du, B. Fan, X. Jin, J. Chi, Fault detection and diagnosis for buildings and HVAC systems using combined neural networks and subtractive clustering analysis, Build. Environ. 73 (2014) 1–11. https://doi.org/10.1016/j.buildenv.2013.11.021.

[31] Y. Guo, J. Wall, J. Li, S. West, Intelligent Model Based Fault Detection and Diagnosis for HVAC System Using Statistical Machine Learning Methods, in: ASHRAE 2013 Winter Conf.,

1286	2013: pp. 1–8.

1287	[32]	S. Li, J. Wen, A model-based fault detection and diagnostic methodology based on PCA

1288	method	and	wavelet	transform,	Energy	Build.	68	(2014)	63–71.

1289	https://doi.org/10.1016/j.enbuild.2013.08.044.

1290	[33]	X. Jin, Z. Du, Fault tolerant control of outdoor air and AHU supply air temperature in VAV

1291	air conditioning systems using PCA method, Appl. Therm. Eng. 26 (2006) 1226–1237.

1292	https://doi.org/10.1016/j.applthermaleng.2005.10.039.

1293	[34]	J. Liang, R. Du, Model-based Fault Detection and Diagnosis of HVAC systems using Support

1294	Vector	Machine	method,	Int.	J.	Refrig.	30	(2007)	1104–1114.

1295	https://doi.org/10.1016/j.ijrefrig.2006.12.012.

1296	[35]	S. Wu, J.Q. Sun, Cross-level fault detection and diagnosis of building HVAC systems, Build.

1297	Environ. 46 (2011) 1558–1566. https://doi.org/10.1016/j.buildenv.2011.01.017.

1298	[36]	W.Y. Lee, J.M. House, N.H. Kyong, Subsystem level fault diagnosis of a building's air-

1299	handling unit using general regression neural networks, Appl. Energy. 77 (2004) 153–170.

1300	https://doi.org/10.1016/S0306-2619(03)00107-7.

1301	[37]	D. Dey, B. Dong, A probabilistic approach to diagnose faults of air handling units in buildings,

1302	Energy Build. 130 (2016) 177–187. https://doi.org/10.1016/j.enbuild.2016.08.017.

1303	[38]	D. Li, Y. Zhou, G. Hu, C.J. Spanos, Optimal Sensor Configuration and Feature Selection for

1304	AHU Fault Detection and Diagnosis, IEEE Trans. Ind. Informatics. 13 (2017) 1369–1380.

1305	https://doi.org/10.1109/TII.2016.2644669.

1306	[39]	S. Li, J. Wen, Application of pattern matching method for detecting faults in air handling unit

1307	system, Autom. Constr. 43 (2014) 49–58. https://doi.org/10.1016/j.autcon.2014.03.002.

1308	[40]	K. Yan, J. Huang, W. Shen, Z. Ji, Unsupervised learning for fault detection and diagnosis of

1309	air	handling	units,	Energy	Build.	210	(2020)	109689.

1310	https://doi.org/10.1016/j.enbuild.2019.109689.

1311	[41]	Y. Yan, P.B. Luh, K.R. Pattipati, Fault diagnosis of HVAC: Air delivery and terminal systems,

IEEE Int. Conf. Autom. Sci. Eng. 2017-Augus (2017) 882–887. https://doi.org/10.1109/COASE.2017.8256214.

[42] C. Zhong, K. Yan, Y. Dai, N. Jin, B. Lou, Energy efficiency solutions for buildings: Automated fault diagnosis of air handling units using generative adversarial networks, Energies. 12 (2019) 1–11. https://doi.org/10.3390/en12030527.

[43] T. Gao, B. Boguslawski, S. Marié, P. Béguery, S. Thebault, S. Lecoeuche, Data mining and data-driven modelling for air handling unit fault detection, E3S Web Conf. 111 (2019). https://doi.org/10.1051/e3sconf/201911105009.

[44] G. Li, Y. Hu, H. Chen, H. Li, M. Hu, Y. Guo, J. Liu, S. Sun, M. Sun, Data partitioning and association mining for identifying VRF energy consumption patterns under various part loads and refrigerant charge conditions, Appl. Energy. 185 (2017) 846–861. https://doi.org/10.1016/j.apenergy.2016.10.091.

[45] N.D. Pham, Q.L. Le, T.K. Dang, HOT aSAX: A novel adaptive symbolic representation for time series discords discovery, Lect. Notes Comput. Sci. (Including Subser. Lect. Notes Artif. Intell. Lect. Notes Bioinformatics). 5990 LNAI (2010) 113–121. https://doi.org/10.1007/978-3-642-12145-6_12.

[46] J. Lin, E. Keogh, S. Lonardi, B. Chiu, A Symbolic Representation of Time Series with Implication for Streaming Algorithms-SAX.pdf, in: DMKD '03 Proc. 8th ACM SIGMOD Work. Res. Issues Data Min. Knowl. Discov., 2003: pp. 2–11.

[47] P.-N. Tan, M. Steinbach, V. Kumar, Introduction to Data Mining, Pearson, Boston, 2005.

[48] R. Agrawal, R. Srikant, Mining Sequential patterns: Generalizations and performance improvements, in: Springer Verlag, 1996: pp. 3–15.

[49] J. Pei, Mining sequential patterns efficiently by prefix-projected pattern growth, in: Int. Conf. Data Eng. (ICDE2001), April, 2001.

[50] J. Pei, J. Han, B. Mortazavi-Asl, J. Wang, H. Pinto, Q. Chen, U. Dayal, M.C. Hsu, Mining sequential patterns by pattern-growth: The prefixspan approach, IEEE Trans. Knowl. Data

1338   Eng. 16 (2004) 1424–1440. https://doi.org/10.1109/TKDE.2004.77.

1339   [51]   M.J. Zaki, SPADE: An efficient algorithm for mining frequent sequences, Mach. Learn. 42

1340   (2001) 31–60. https://doi.org/10.1023/A:1007652502315.

1341   [52]   J. Ayres, J. Flannick, J. Gehrke, T. Yiu, Sequential pattern mining using A bitmap

1342   representation, Proc. ACM SIGKDD Int. Conf. Knowl. Discov. Data Min. (2002) 429–435.

1343   https://doi.org/10.1145/775107.775109.

1344   [53]   J. Pei, J. Han, W. Wang, Mining sequential patterns with constraints in large databases, Int.

1345   Conf. Inf. Knowl. Manag. Proc. (2002) 18–25. https://doi.org/10.1145/584796.584799.

1346   [54]   Y.-L. Chen, T.-K. Huang, Discovering fuzzy time-interval sequential patterns in sequence

1347   databases, IEEE Trans. Syst. Man, Cybern. Part B. 35 (2005) 959–972.

1348   [55]   Y. Hirate, Generalized Sequential Pattern Mining with Item Intervals, 1 (2006) 51–60.

1349   [56]   Y.-L. Chen, M.-C. Chiang, M.-T. Ko, Discovering time-interval sequential patterns in

1350   sequence   databases,   Expert   Syst.   Appl.   25   (2003)   343–354.

1351   https://doi.org/https://doi.org/10.1016/S0957-4174(03)00075-7.

1352   [57]   F.J. Martínez-De-Pisón, A. Sanz, E. Martínez-De-Pisón, E. Jiménez, D. Conti, Mining

1353   association rules from time series to explain failures in a hot-dip galvanizing steel line,

1354   Comput. Ind. Eng. 63 (2012) 22–36. https://doi.org/10.1016/j.cie.2012.01.013.

1355   [58]   F.J. Martínez-de-Pisón Ascacíbar, A. Pernía Espinoza, F. Martínez, Roberto, R. Escribano

1356   García, P. Guillén Rondón, D. Conti Guillén, System for uncovering hidden knowledge in real

1357   time for the analysis of environmental and agricultural processes, XIII Int. Conf. Proj. Eng.

1358   (2009).

1359   [59]   G. Kaur, Association Rule Mining: A survey, Int. J. Comput. Sci. Inf. Technol. 5 (2014) 2320–

1360   2324.

1361   [60]   T.M. Therneau, E.J. Atkinson, An introduction to recursive partitioning using the rpart

1362   routines, 1997.

1363   [61]   A. Capozzoli, M.S. Piscitelli, S. Brandi, D. Grassi, G. Chicco, Automated load pattern learning

1364   and anomaly detection for enhancing energy management in smart buildings, Energy. 157

1365   (2018) 336–352. https://doi.org/10.1016/j.energy.2018.05.127.

1366 [62] R.K. Pearson, Data cleaning for dynamic modeling and control, Eur. Control Conf. ECC 1999

1367   - Conf. Proc. (2015) 2584–2589. https://doi.org/10.23919/ecc.1999.7099714.

1368 [63] S. Li, A Model-Based Fault Detection and Diagnostic Methodology for Secondary HVAC

1369   Systems, Drexel Univ. (2009).

1370 [64] M. Kim, S.H. Yoon, P.A. Domanski, W. Vance Payne, Design of a steady-state detector for

1371   fault detection and diagnosis of a residential air conditioner, Int. J. Refrig. 31 (2008) 790–799.

1372   https://doi.org/10.1016/j.ijrefrig.2007.11.008.

1373 [65] C.W. Roh, M. Kim, H.S. Kim, M.S. Kim, Design Method Of Steady State Detector For Multi-

1374   Evaporator Heat Pump System With Decomposition Analysis Technique, (2010).

1375 [66] C. Miller, Z. Nagy, A. Schlueter, A review of unsupervised statistical learning and visual

1376   analytics techniques applied to performance analysis of non-residential buildings, Renew.

1377   Sustain. Energy Rev. 81 (2018) 1365–1377. https://doi.org/10.1016/j.rser.2017.05.124.

1378 [67] A. Dexter, J. Pakanen, Demonstrating Automated Fault Detection and Diagnosis Methods in

1379   Real Buildings, in: Proc. VTT Symp. 217, 2001: p. 381. https://doi.org/951-38-5725-5.

1380 [68] M. Charrad, N. Ghazzali, V. Boiteau, A. Niknafs, NbClust: An R Package for Determining the

1381   Relevant Number of Clusters in a Data Set Malika, J. Stat. Softw. 61 (2014).

1382   https://doi.org/10.18637/jss.v061.i06.

1383 [69] R Core Team, R: A Language and Environment for Statistical Computing, (2017).

1384   http://www.r-project.org/.

1385 [70] M. Hahsler, B. Grun, K. Hornik, arules – A Computational Environment for Mining

1386   Association Rules and Frequent Item Sets, J. Stat. Softw. 14 (2005) 1–6.

1387   papers2://publication/uuid/388D2132-AF39-463F-8D87-91A45FA1E26D.

1388 [71] S. Ahmad, S. Purdy, Real-Time Anomaly Detection for Streaming Analytics, (2016).

1389   http://arxiv.org/abs/1607.02480.

Appendix A

Table A. Discretization intervals for all the analysed variables.

Variable	ID	Unit	Sym. A	Sym. B	Sym. C	Sym. D	Sym. E
SF_WAT	1	[W]	< 522 **OFF**	522 – 1265 **ON**	1265 – 2440 **ON**	> 2440 **ON**	-
RF_WAT	2	[W]	< 181 **ON**	181 - 337 **ON**	336 – 502 **ON**	> 502 **ON**	-
SA_CFM	3	[m³/h]	< 591 **OFF**	591 – 2276 **ON**	2276 – 3414 **ON**	3414 – 4706 **ON**	> 4706 **ON**
RA_CFM	4	[m³/h]	< 838 **OFF**	838 – 2712 **ON**	2712 – 3527 **ON**	> 3527 **ON**	-
OA_CFM	5	[m³/h]	< 477 **ON**	477 – 1146 **ON**	> 1146 **ON**	-	-
SA_TEMP	6	[°C]	< 15,9 **ON**	15,9 – 23,5 **ON**	23,5 – 32,4 **ON**	> 32,4 **ON**	-
MA_TEMP	7	[°C]	< 20,3 **ON**	20,3 – 30,8 **ON**	> 30,8 **ON**	-	-
RA_TEMP	8	[°C]	< 25,7 **ON**	25, 7 – 31,5 **ON**	>31,5 **ON**	-	-
HWC_DAT	9	[°C]	< 20,2 **ON**	20,2 – 26 **ON**	26 – 35,7 **ON**	> 35,7 **ON**	-
CHWC_DAT	10	[°C]	< 14,4 **ON**	14,4 – 22 **ON**	22 – 30,7 **ON**	> 30,7 **ON**	-
SF_DP	11	[Pa]	< 324 **OFF**	324 – 562 **ON**	562 – 770 **ON**	> 770 **ON**	-
RF_DP	12	[Pa]	< 46 **ON**	46 – 114 **ON**	> 114 **ON**	-	-
SF_SPD	13	[%]	< 50 **OFF**	50 – 67 **ON**	67 – 75 **ON**	75 – 87 **ON**	> 87 **ON**
RF_SPD	14	[%]	< 30 **OFF**	30 – 43 **ON**	43 – 57 **ON**	57- 69 **ON**	> 69 **ON**
OA_TEMP	15	[°C]	< 18,3 **ON**	> 18,3 **ON**	-	-	-
CHWC_EWT	16	[°C]	< 1,3 **ON**	1,3 – 2,8 **ON**	2,8 – 6,7 **ON**	> 6,7 **OFF**	-
CHWC_LWT	17	[°C]	< 13,3 **ON**	13,3 – 19,9 **ON**	19,9 – 21,2 **ON**	> 21,2 **OFF**	-
CHWC_GPM	18	[m³/h]	< 0,9 **ON**	0,9 – 1,7 **ON**	> 1,7 **ON**	-	-
E_ccoil	19	[kW]	< 11,7 **ON**	> 11,7 **ON**	-	-	-
CHWC_VLV	20	[%]	< 41 **ON**	41 – 75 **ON**	> 75 **ON**	-	-
EA_DMPR	21	[%]	< 20 **ON**	20 – 70 **ON**	> 70 **ON**	-	-
OA_DMPR	22	[%]	< 20 **ON**	20 – 47 **ON**	47 – 77 **ON**	> 77 **ON**	-
RF_SST	23	[-]	< 0,5 **OFF**	> 0.5 **ON**	-	-	-

Table A summarizes the transformation results obtained, with the specification of the numerical range

corresponding to each symbol for all the analysed operational variables.

Table B. Most representative extracted temporal association rules.

ID N°	Antecedent	Consequent	Supp.	Conf.	ACTUAL TIME LAG	SUPP. DAY FAULTY
1077	SF_SPD [A-B], EA_DMPR [A-B], RF_WAT [A-B]	CHWC_DAT [B-A]	0.70	0.8	15	0.27
1078	SF_WAT [A-B], EA_DMPR [A-B], RF_WAT [A-B]	CHWC_DAT [B-A]	0.70	0.8	15	0.27
1526	SF_SPD [A-B], EA_DMPR [A-B], RF_WAT [A-B]	CHWC_DAT [B-A], CHWC_LWT [B-A]	0.70	0.8	15	0.27
1527	SF_WAT [A-B], EA_DMPR [A-B], RF_WAT [A-B]	CHWC_DAT [B-A], CHWC_LWT [B-A]	0.70	0.8	15	0.27
1864	SF_SPD [A-B], EA_DMPR [A-B], RF_WAT [A-B]	CHWC_DAT [B-A], CHWC_LWT [B-A], SA_TEMP [B-A]	0.75	0.8	15	0.27
1865	SF_WAT [A-B], EA_DMPR [A-B], RF_WAT [A-B]	CHWC_DAT [B-A], CHWC_LWT [B-A], SA_TEMP [B-A]	0.75	0.8	15	0.27
8661	RF_SPD [A-B], CHWC_LWT [C-B], EA_DMPR [A-B]	CHWC_DAT [B-A], RF_SPD [B-C]	0.9	1	30	0.09
8750	RF_SPD [A-B], EA_DMPR [A-B], RF_SST [A-B]	CHWC_DAT [B-A], RF_SPD [B-C]	0.8	0.89	30	0
6255	RF_SPD [A-B], CHWC_LWT [C-B], RA_CFM [A-B]	CHWC_DAT [B-A], RF_SPD [B-C], CHWC_LWT [B-A]	0.89	0.8	15	0.18
6256	RF_SPD [A-B], CHWC_LWT [C-B], RF_SST [A-B]	CHWC_DAT [B-A], RF_SPD [B-C], CHWC_LWT [B-A]	0.89	0.8	15	0.09
6226	RF_SPD [A-B], CHWC_LWT [C-B], RF_SST [A-B]	CHWC_DAT [B-A], RF_SPD [B-C], SA_TEMP [B-A]	0.89	0.8	15	0.09
6936	RF_SPD [A-B], CHWC_LWT [C-B]	CHWC_DA T [B-A], RF_SPD [B-C], SA_TEMP [B-A]	0.889	0.8	15	0.18
1933	SF_SPD [A-B], EA_DMPR [A-B], RF_WAT [A-B]	CHWC_LWT [B-A], SA_TEMP [B-A]	0.75	0.8	15	0.27
1934	SF_WAT [A-B], EA_DMPR [A-B], RF_WAT [A-B]	CHWC_LWT [B-A], SA_TEMP [B-A]	0.75	0.8	15	0.27
5257	RF_SPD [A-B], EA_DMPR [A-B], RA_CFM [A-B]	RF_SPD [B-C]	0.82	1	30	0.18
5259	RF_SPD [A-B], EA_DMPR [A-B], RF_SST [A-B]	RF_SPD [B-C]	0.82	1	30	0.09
6415	RF_SPD [A-B], CHWC_LWT [C-B], RF_WAT [A-B]	RF_SPD [B-C], CHWC_LWT [B-A]	0.8	0.8	15	0.09
6416	RF_SPD [A-B], CHWC_LWT [C-B], RF_DP [A-B]	RF_SPD [B-C], CHWC_LWT [B-A]	0.8	0.8	15	0.09
6126	RF_SPD [A-B], CHWC_LWT [C-B], RF_WAT [A-B]	RF_SPD [B-C], CHWC_LWT [B-A], SA_TEMP [B-A]	0.89	0.8	15	0.09
8309	RF_SPD [A-B], CHWC_LWT [C-B], EA_DMPR [A-B]	RF_SPD [B-C], CHWC_LWT [B-A], SA_TEMP [B-A]	0.78	0.78	15	0.09
15268	RF_SPD [A-B], EA_DMPR [A-B], RF_WAT [A-B]	RF_SPD [B-C], SA_TEMP [B-A]	0.8	0.89	30	0
15269	RF_SPD [A-B], EA_DMPR [A-B], RF_DP [A-B]	RF_SPD [B-C], SA_TEMP [B-A]	0.8	0.89	30	0
1253	**SF_SPD [A-B], EA_DMPR [A-B], RF_WAT [A-B]**	**SA_TEMP [B-A]**	**0.70**	**0.8**	**15**	**0.27**
1254	SF_WAT [A-B], EA_DMPR [A-B], RF_WAT [A-B]	SA_TEMP [B-A]	0.70	0.8	15	0.27
1406	SF_WAT [A-B], EA_DMPR [A-B], RF_WAT [A-B]	CHWC_DAT [B-A], SA_TEMP [B-A]	0.70	0.8	15	0.27
5240	CHWC_EWT [D-C], EA_DMPR [A-B], RF_WAT [A-B]	CHWC_DAT [B-A], SA_TEMP [B-A]	0.70	0.8	30	0.27

1396

1397 Table B reports 26 rules (two for each unique consequent transaction) extracted from the transient

1398 dataset with the specification of the event chains of antecedent and consequent, the value of support

1399   and confidence within the ACTUAL TIME LAG and its duration (evaluated on the training dataset),

1400   and the SUPP.DAY$_{\text{FAULTY}}$ (evaluated on the testing dataset).